WOODS HOLE OCEANOGRAPHIC INSTITUTION

Woods Hole, Massachusetts

Reference No. 54-5

MARINE METEOROLOGY

The Erosion of Cumulus Towers

By
Joanne Starr Malkus
and
R. S. Scorer

January 1954

APPROVED FOR DISTRIBUTION _____
Director

Abstract

The laws established by Davies and Taylor (1950) for the rise of air bubbles in liquid have been modified to apply to buoyant air bubbles in air. In addition, a simple law for the erosion of these buoyant air bubbles has been proposed. An erosion parameter, E, is derived in terms of these laws which, if they are valid, should be constant for all isolated bubbles. The erosion constant has been expressed in terms of the bubble's upward velocity and acceleration and its buoyancy. The theory is thus subject to test in the case of cumulus towers by simple measurements from time-lapse motion pictures and an environment temperature sounding.

Observations of eleven relatively isolated cumulus bubbles selected from both trade-wind region and middle latitudes show that E is indeed constant within the limits of measurement. A case of the aggregation of several small bubbles into a larger one is also studied, and the applicability to it of the same erosion and drag laws established. The interaction of bubbles with one another and with the environment to form large cumulus clouds is discussed qualitatively.

I. INTRODUCTION

The first quantitative model of cumulus cloud growth was the so-called "parcel method", which predicted accelerations, velocities, lapse rates within, and levels attained by convective elements from the external sounding and a thermodynamic diagram. The parcel was assumed not to interact in any way with the surrounding air. When at the time of World War II observations of individual cumulus clouds became available, it was recognized that the parcel method was seriously inadequate due to this assumption of non-interaction and that on a given day, the majority of cumuli terminated far below the level predicted from parcel considerations. Furthermore, airplane measurements revealed that the lapse rate within clouds was generally steeper than moist adiabatic and fluctuating, while liquid water contents usually fell far below that anticipated.

As a consequence of these observations, the next important step in cumulus study was taken by Stommel (1947), who proposed that a cloud in its ascent was continually mixing with the drier air of its surroundings. He devised a thermodynamic method to calculate the amount of this mixing or "entrainment" from soundings made nearly simultaneously within and outside a cloud. In so doing he proposed an analogy between a cumulus and a jet of fluid injected into a resting environment. He dealt with a rising column which was in a steady state and which was internally well mixed or homogeneous. Models based on entrainment have been extended by others (their work is reviewed by Malkus, 1952a) and have shed light on many important features of cumulus clouds, such as their failure to reach parcel heights, their slopes and asymmetries in a shearing wind field, and their transports of heat, moisture, and momentum.

Useful as the entrainment model has been, however, it too fails to give information beyond a certain point. The analogy between a fluid hose injected into a resting tankful of water and a cumulus must not be pushed too far. It is well known that convective "jets" in the atmosphere are self-initiating and self-maintaining, and that they grow from rest and eventually decay. The entrainment model, since it has so far been concerned with steady drafts, has been unable to inquire about the time dependence or life cycle of a cloud. Furthermore, the actual mechanism by which entrainment occurs has been deliberately circumvented by the use of a homogeneous draft discontinuously distinct from the surroundings, and only the effects of mixing have been considered. It has been tacitly assumed that eddying or turbulence plays an important role in entrainment, though a considerable amount of rather unproductive argumentation has gone on concerning how much of the influx may be ordered convergence.

Recently, a model of cumulus was suggested by Scorer and Ludlam (1953) which, if quantitatively establishable, surmounts the foregoing difficulties, simultaneously introducing time dependence and providing a mechanism for the entrainment process. The new model envisages a cumulus as an aggregate of buoyant bubbles of saturated air, which interact both temporally and spatially. The buoyancy of an individual bubble is nearly balanced by the drag caused by the deflection and flow of outside air around the spherical cap, so that its velocity of ascent is prevented from approaching anywhere nearly that of the _ ly accelerating parcel. The model envisages that the bubble continuously sheds its outer skin as it rises, while maintaining the quasi-spherical shape of its upper surface, until finally its life ends when it has been completely wasted away by erosion.

Behind the flattened bubble cap is formed a turbulent wake, which is composed of a mixture of the saturated air shed from the bubble and air from the surroundings which has been incorporated into the wake. The eddy stresses within the wake transform the potential energy released by the bubble's ascent into turbulent energy in the air behind it. The wake thus consists of rough, slowly ascending buoyant air with properties somewhere between those of the undiluted bubble cap and those of the surroundings. It thus constitutes a preferred region for the ascent of succeeding bubbles, protecting them from erosion by the environment.

The model further hypothesizes that large cloud bubbles (see Ludlam and Scorer, 1953) are formed by the aggregation of smaller ones and their wakes, and that a cloud that penetrates to great heights generally does so by the successive release of single bubbles. These emerge beyond the region of protection by surrounding cloud mass as isolated towers. The initial formation and maintenance of a cumulus may occur in different ways, depending on location, and external conditions. A succession of bubbles may enter through cloud base, originating from thermals in the subcloud layer, or the cloud-scale bubbles may form entirely within the cloud layer, usually at any level up to that where the environment lapse rate becomes more stable than moist adiabatic, called the "tectonic limit" by Scorer and Ludlam (1953).

Many features of this model are supported qualitatively by observations already existing; among these is the growth of large cumuli by successive tower production (Byers and Battan, 1949), the aggregation of smaller cloud elements to form larger ones (Malkus, 1953), and others such as the rounded tops of growing cumuli which are common visual observations.

Perhaps the most promising feature of the bubble model is, however, that it points to the unit or "proton" of convection, the mechanics and life cycle of which may possibly be described analytically. If so, the way is paved for building up a cumulus by a series of interacting bubbles. The primary purpose of this paper is to formulate the laws governing the rise and erosion of a single, non-interacting saturated bubble and to test these by observations upon isolated cumulus towers. It is assumed here that the erosion of individual isolated bubbles depends simply on a few parameters and is independent of properties of the environment other than lapse rate. The role of the environment is held critical in the interaction of bubbles to constitute a cloud. Preliminary steps toward the aggregation of smaller bubbles into larger ones are taken in the later sections.

II. THE THEORETICAL MODEL

a. A Differential Equation for the Rate of Rise of Cumulus Bubbles

Based on the work of Davies and Taylor (1950), who studied the rise of air bubbles in liquid, a differential equation for vertical velocity as a function of time is derived which may be shown applicable to isolated cloudy bubbles. Davies and Taylor investigated, both theoretically and experimentally, bubbles of total angular aperture ($2\theta_m$ in Fig. 19) ranging from about 70°-120°. They showed that the upper surfaces of these bubbles were spherical to a very high degree of approximation and that the flow around these spherical caps was, within small experimental error, the same as potential flow around a sphere. The velocity derived from the appropriate potential function was found to agree with the measured constant velocities of the

bubbles' ascent. Each bubble was found also to retain its shape and spherical surface throughout its rise.

The condition that a spherical shape be an equilibrium configuration for a rising bubble is that the total pressure be constant along the curved surface. The model of Davies and Taylor is illustrated in Fig. 1. The frame of reference is shifted so that the bubble is held at rest and the air has a free stream velocity w_0 past the bubble, where w_0 is its constant ascent speed. At the stagnation point, O, the dynamic pressure $\frac{1}{2}\rho w_0^2$ must be exactly balanced by the difference in static pressure exerted by the column within the bubble beneath O and that by an equivalent outside column, i.e. the buoyancy and drag are equal. This balance maintains at every point along the curve B if

$$gBx = \frac{1}{2}\left(w_0^2 \frac{9}{4}\sin^2\theta\right) \tag{1}$$

where the left side represents the decrease in static pressure from O to any point A at an angle θ and the right side represents the decrease in dynamic pressure. The quantity in the parenthesis, $w_0^2\ 9/4\ \sin^2\theta$, is the square of the velocity at A, derived from the potential function for a sphere at rest in a fluid with undisturbed velocity w_0. The acceleration of gravity is denoted by g and the buoyancy of the bubble by B, where $B = \rho - \rho_1/\rho$; ρ_1 is the bubble density and ρ that of the surroundings.

Referring again to Figure 1, we see that

$$x' = x\cos\theta = R\cos\theta\ (1 - \cos\theta) \tag{2}$$

and therefore

$$gBR = w_o^2 \frac{9}{8} \frac{\sin^2 \theta}{\cos \theta (1 - \cos \theta)} \cong \frac{9}{4} w_o^2 \quad \text{for small } \theta \tag{3}$$

The approximation for small θ holds within 10% if θ is as large as 30°. Finally we have

$$w_o = \frac{2}{3} (gBR)^{\frac{1}{2}} \tag{4}$$

This is the relation checked experimentally by Davies and Taylor (1950) when $B \sim 1$. The fact that the measured w_o and the w_c calculated using the measured R agreed so well indicated the validity of the assumption of potential flow around the cap.

Equation (3) may be rewritten

$$gB = \frac{9}{4R} w_o^2 \tag{5}$$

which shows the balance of forces per unit mass achieved when the bubble has its limiting or equilibrium velocity w_o. The left-hand term gB is the buoyancy force per unit mass and the right-hand term is the drag force per unit mass, this force being called pressure or form drag by hydrodynamicists. Since the mass of the bubble is proportional to R^3, the form drag force on the bubble is proportional to R^2 or to its surface area, as expected.

Taylor (1950) applied these results to a buoyant air bubble in air in the case of the atomic bomb cloud. He showed that the measured rate of rise of the cloud was very nearly equal to that calculated using equation (4) treating the bubble as one of zero density with an equivalent radius equal to that at which $\rho_1 = \rho_o/2$. The relation between ρ_1, the bubble density

and ρ_o of the environment he found from other considerations involving the bomb. An atomic bomb cloud shown side by side with a single trade cumulus bubble is depicted in Figure 2. In modifying Taylor's results to construct a model for isolated cumulus bubbles, the following basic assumptions are employed: first, that the caps (cloud tower tops) are quasi-spherical and second that the actual rate of rise, w, departs not too widely from w_o, so that the same drag law will be applicable. In this case, the forces are not quite balanced and an acceleration term is introduced so that we have a differential equation for w as a function of time, namely

$$\frac{dw}{dt} = gB - \frac{9}{4R} w^2 \qquad \text{or}$$

$$\frac{dw}{dt} + \frac{9}{4R} w^2 = gB \qquad (6)$$

where the acceleration is now set equal to the sum of the forces per unit mass, these being buoyancy and form drag.

The model for a cumulus tower is not yet complete, however, for in general R is not constant as in the case of Davies and Taylor, but is decreasing with time due to erosion. This decrease in size, in fact, is envisaged as the reason for introduction of the acceleration term in the atmospheric case. The bubbles are supposed to retain their shape as they erode and maintain a nearly constant aperture, the decrease in mass being reflected in a decreasing R. As R decreases, w_o, the limiting velocity, also decreases according to (4), so that the actual cloudy bubble is always rising slightly faster than w_o and decelerating. The major new assumption

of the present paper is the introduction of an erosion law, or a functional dependence of R upon t.

b. The Erosion of a Bubble

The physical mechanism of erosion is envisaged as follows: The surface of the bubble cap represents an unstable interface between two fluids. Similarly in the case where water is poured on the top of kerosene, the instability will attempt to relieve itself by the growth of protuberances upward from the lighter fluid through the interface. In the case of the cloud, these give the tower a knobbly or cauliflower-like appearance superposed upon the spherical cap. The protuberances will mix with the environment and by dilution and evaporation become more dense than the tower. They will thus sink relative to the cap and be swept back by the ambient flow and incorporated into the wake. The bubble cap is thus hypothesized to retain its shape and bubbles of all sizes are assumed geometrically similar. If this hypothesis is valid, it may be possible to set forward an erosion law which holds for all isolated bubbles. An extremely simple erosion law is tested here. The rate of erosion of volume is hypothesized to depend only upon the surface area and the buoyancy which is responsible for the erosion, namely

$$\frac{dR^3}{dt} = - 3ER^2 gB \tag{7}$$

where the constant of proportionality is called 3E, or

$$\frac{dR}{dt} = - EgB \tag{8}$$

and we wish to determine whether E, a measure of the rate of erosion, is the same for all bubbles. We can expect E to be a constant only for bubbles rising into undisturbed surroundings, but it is just such bubbles that are most readily observed as rising cumulus towers.

The implications of the introduction of so simple an erosion law must indeed be examined. It should especially be inquired why w to some power was not explicitly included, for its omission carries the inference that for the range of velocities possessed by convective bubbles, the erosion should be quite independent of the flow around the bubble and depend only upon buoyancy and surface area. Although a more general law for erosion is discussed in Appendix I, the simple one of equation (7) may be subjected to observational test. Since the validity of the erosion law is the crux of the development in this paper, the major part of the observational section is directed towards its testing in actual cases.

In order to make these tests, the erosion law of equations (7) and (8) is to be combined with the equation of motion, equation (6). If we consider equation (8) under conditions of constant buoyancy, as when the external lapse rate is close to the wet adiabatic, then

$$R = - EgBt \qquad (9)$$

if we take t = 0 at the moment of exhaustion of the bubble and negative t everywhere before that during its rise. Then after substituting (9) for R equation (6) becomes

$$\frac{dw}{dt} + \frac{9}{4EgB\,(-t)}\,w^2 = gB \qquad (10)$$

This equation is a non-linear differential equation of the Riccati-type. It is not readily integrated (see Ince, 1944, p. 23) but may be easily transformed into a linear, second-order equation with non-constant coefficients, which is also not readily integrated. This, however, does not constitute a serious misfortune. Equation (10) may be readily solved for E, giving

$$\frac{3}{2} E^{-\frac{1}{2}} \equiv G = \frac{(-t)^{\frac{1}{2}} gB (1 - \dot{w}/gB)^{\frac{1}{2}}}{w} \tag{11}$$

where henceforth dw/dt will be written $\dot{w}$. Since the purpose of this analysis is to test whether the combined force and erosion laws are valid, that is whether E is constant for all isolated cloud bubbles, the equation will be used for the present in the form (11). It is noteworthy that this equation provides an estimate of E from the most easily observable quantities, viz. the height of the bubble as a function of time and the buoyancy. It does not involve a measurement of R which, at this stage, we do not know how to measure precisely and is usually difficult to estimate because of the knobbly appearance of cumulus tower tops. Also (9) will provide an estimate of R which must be consistent with observation if the theory is valid.

In general, the buoyancy of a saturated cumulus bubble will not be constant, since the environment lapse rate usually differs from moist adiabatic. The effects of buoyancy variations will be investigated in general in Appendix I. There it is shown that if such variations in gB are slow, equation (11) is still applicable using the variable values of buoyancy. This result may be established very simply in one special case, namely if the buoyancy variation may be expressed by a function of the form

$$B = B_0 e^{\alpha t} \tag{12}$$

Thus from (8)

$$R = EgB_0 \alpha^{-1} (1 - e^{\alpha t}) \tag{13}$$

and

$$\frac{3}{2} E^{-\frac{1}{2}} \cong G = \left(\frac{e^{-\alpha t} - 1}{\alpha}\right)^{\frac{1}{3}} \frac{gB (1 - \dot{w}/gB)^{\frac{1}{2}}}{w} \tag{14}$$

If the buoyancy increases by one-third in 100 seconds, then $\alpha t \approx 0.3$ and

$$\frac{e^{-\alpha t} - 1}{\alpha} = \left(- t + \frac{1}{2} \alpha t^2 - \ldots\right) \approx - t$$

in which case (14) reduces to (11) except that B is now a variable. This means that (11) can be used by putting in the buoyancy at each instant, unless the changes are somewhat larger than those just indicated. This conclusion is derived more generally in the Appendix and will be used throughout the observational work.

c. Critical Discussion of the Theoretical Model and its Applicability to Cloud Towers

The theoretical model may be divided into two essential parts, the force law and the erosion law. The erosion law is strictly an assumption, the applicability of which to cumulus towers is only to be established by observation. The applicability of the force law, on the other hand, may be established theoretically, subject only to two conditions: first that the cloud towers retain a quasi-spherical upper surface, and second that the erosion is

sufficiently slow so that the ascent velocity does not radically depart from
the limiting value w_0. The meaning of the latter assumption is that the flow
pattern around the tower is quasi-steady, or that the streamline picture
changes from a steady-state configuration characteristic of one limiting ve-
locity to that of another without large transient terms. The exact differ-
ential equation could be found by starting from the equations of unsteady
potential flow and the result would be some factor slightly greater than
one to multiply by the $\dot{w}$ term in equation (6). This factor arises physi-
cally from the fact that an additional acceleration must be produced by the
buoyancy to deflect and send backward a small film of environment air sur-
rounding the bubble. Another correction to the acceleration term, in the
opposite sense, may be caused by the emergence and shedding of the buoyant
protuberances from the cap which may give a small "rocket effect". Since
these are both second-order corrections and opposite in sense, they will
be neglected. The measurements now available, anyhow, would not permit an
observational test accurate enough to select between a factor of one times
the $\dot{w}$ term in equation (11) and a factor of about 1.3.

The applicability of equation (6) to cloud towers may be further vali-
dated in two ways, without building upon the work of Davies and Taylor, pro-
vided only that the tops are quasi-spherical. At Reynolds numbers of 10^6
and higher (for cloud tower Rs = 10^8 - 10^9) experiments on turbulent flow
around all types of spheres, ranging from gaseous to solid (see Goldstein,
Vol. I, 1938, p. 25) have shown that up to 30° angles on either side of the
flow axis, the ambient velocity distribution is indistinguishably different
from potential flow. Up to angles of 60°, the flow closely approximates
potential flow. Furthermore, we may check the drag law in another way.

According to the theoretical analysis

$$\frac{\text{Drag force}}{\text{unit mass}} = \frac{9}{4R} w^2 \tag{15}$$

or

$$F_D = \frac{9}{4R} M w^2 \tag{16}$$

where F_D is the drag force on the tower; M is its mass; and R its radius of curvature. Equation (16) may be compared with the form drag equation commonly used in the study of turbulent flow around spheres by hydrodynamicists, namely

$$F_D = A_c \frac{1}{2} C_D \rho w^2 \qquad \text{or} \tag{17}$$

$$C_D = 2 F_D / A_c \rho w^2$$

where A_c is the cross-sectional area of the sphere; ρ is the fluid density; and C_D is a dimensionless drag coefficient, found experimentally to depend upon Reynolds number.

We may use (16) to obtain an expression for F_D and then apply (17) to get C_D. The mass of a bubble with half-aperture θ_m and radius of curvature R is

$$M = \frac{2 \pi R^3}{3} \rho \left[1 - \cos \theta_m \left(1 + \frac{1}{2} \sin \theta_m \right) \right] \tag{18}$$

while its cross-sectional area is

$$A_c = \pi R^2 \sin^2 \theta_m \tag{19}$$

The average angular half-aperture of observed cloudy bubbles came out 30°. In this case C_D is found to be 0.24.

In experiments on turbulent flow around spheres, at Reynolds numbers 10^6 and above, C_D comes out 0.20 (see Rouse, 1938, p. 215).

Thus our entire theoretical model could have been constructed merely from the common observation that the tops of cumulus towers are almost spherical. The differential equation could be set up using a w^2 drag law with a $C_D = 0.20$ and a buoyancy acceleration, gB, with the erosion law introduced specifying A_c as a function of time. An equation similar to (11) would thus result which would contain a constant proportional to E. The observational testing would be entirely the same as that which follows. Taylor's model, however, and the bubble approach used here are preferred because more is thus said about mechanism, both concerning the maintenance of the spherical cap and the production of the turbulent wake.

The modifications which may be expected in a shearing wind field are discussed in Appendix II.

III. OBSERVATIONS ON CUMULUS TOWERS

The primary purpose of the observational work is to test the constancy of E in equation (11). A superficial examination of time-lapse photographs reveals many cumulus towers sufficiently isolated for the equation to be applicable to them. A bubble is suitable only if its motion is not much affected by the ascent of a larger one beneath, which subsequently overtakes it. This applies not only to a separate large bubble but also to the wake

of the bubble itself; and the demise of a bubble must be noted not only by
a cessation of ascent but also by a disappearance of the clear-cut top. The
wake usually continues to ascend for several seconds after the bubble itself
is exhausted, but owing to evaporation its outline is not clear and its size
is shrinking. When there is considerable wind shear, a bubble is carried to
one side, and is therefore not interfered with by its successors; and when
the surroundings are dry the evaporation of the wake prevents interference
by it. Indeed these two conditions which militate against the growth of
clouds because they isolate the bubbles and prevent successors from adding
to their wakes, are ideal for the study of individual bubbles.

It was envisaged (by Scorer and Ludlam) that a bubble would be composed
by aggregation of several smaller ones. This process has been observed in
the trade-wind region and described qualitatively by Malkus (1953). The com-
posite nature of the large bubbles used in the present study was apparent
from the time-lapse films. In general, the uppermost visible part of a ris-
ing tower ascends somewhat irregularly, while the upper limit of a smoothed
outline ascends with a more slowly varying speed. It is sometimes possible
to make measurements both on the bubble as a whole and on the individual
ones of which it is composed, if at any time they emerge from the top long
enough to make an ascent alone in the clear air. It is significant that
equation (11) has been applied successfully both to composite and to indi-
vidual bubbles, and this strengthens the contention that the theory des-
cribes a real process, and that not only are cloudy bubbles built up from
several smaller ones, but that we may treat the composite ones just like
the individuals. After discussing the measurements on several cases of

isolated single bubbles, a case of aggregation of several of these individuals into a composite bubble is considered.

The time-lapse motion pictures used were made on field programs of cumulus study by the marine meteorology group of the Woods Hole Oceanographic Institution. A group of films was used from the Nantucket program of the summer of 1950 (see Malkus and Bunker, 1952; Malkus, 1952b; also Malkus and Stern, 1953) and another group from the Caribbean expeditions of 1952 and 1953 (described in part by Malkus, 1953). The measurements were made by projecting the films in a microfilm reader. The height of the cloud base was known from airplane observations (usually of the same clouds being photographed, while the photography was in progress) and the cloud top height was derived from the height of it and the base above the horizon. Errors due to the earth's curvature and to the height of the camera above sea level were found to be negligible. The height of each tower was plotted against time (the camera shutter was automatically tripped at a fixed interval) and a curve was drawn to smooth out the irregularities produced by the knobbly surface of the tower.

The vertical velocity was drawn to be reduced to zero at the end of each ascent, but since we are concerned with the velocity relative to the air, and the air may have been ascending slowly above the buoyant wake, it is likely that the deceleration of the bubble in its final stages has been overestimated, though the velocity would not be seriously affected. This would lead to an overestimation of G in the last second or so, which is indeed observed in many cases.

Theoretically, examination of equation (6) tells us the same thing.

It is clear that w cannot go to exactly zero at t = 0 if gB is to remain positive. Physically, this means that the bubble, since it is decreasing in size, must always rise with a velocity slightly in excess of its limiting velocity. Although the limiting velocity goes to zero at t = 0, the actual velocity of what is left of the bubble must remain greater than zero.

Altogether, eleven cases of individual bubbles were studied; in nine of these the environment lapse rate was such that a constant value of buoyancy could be used. In one of the latter, the bubble studied was so isolated that it seemed to behave in every way like the "ideal" bubble described by the model. Therefore, this case, that of a cloud over Nantucket, U.S.A. on August 14, 1950, will be described first and in greater detail than most of the others.

a. Case of August 14, 1950. Nantucket, U.S.A.

The clouds formed on this day have been discussed at length elsewhere (Malkus and Bunker, 1952; Malkus, 1952b; Malkus and Stern, 1953), and vast amounts of supplementary data were available. The cloud studied is shown in a sequence from the film in Figure 3. The bubble selected is the topmost forming the cloud turret and is indicated by the white arrow. The wind shear on this day was so high (-5 mps/km) that successive bubbles were unable to interact and the cloud tower petered out at a height where the environment lapse rate still exceeded moist adiabatic.

The measurements from the time-lapse films are shown in Figure 4. The points give the height of the bubble cap at each frame (3 seconds apart) beginning when the bubble emerges from the cloud, or when the white arrow first appears on Figure 3, until it reached nearly its maximum height and

the film showed its edges becoming fuzzy. At this frame, as nearly as it could be specified, t was set equal to zero. A smooth curve is drawn through these points on Figure 4 and observations read off every four points, or twelve seconds apart. Velocities are found by taking first differences of these heights and accelerations by taking second differences. These second differences are indicated by x's in the inset graph of Figure 4, converted into cm/sec^2, and a smooth curve is drawn through them. The accelerations used in the table below are taken from the smoothed curve, and the velocities are usually smoothed in a similar manner. If the buoyancy B is taken as a constant equal to 0.0836 (to be discussed presently), the value of G comes out for each observation as shown in Table I.

The buoyancy of the bubble was estimated from the clear air sounding according to the following procedure: the temperature curve followed by the bubble was assumed to be the moist adiabat crossing the sounding curve at the bubble's level of origin. From this, its virtual temperature excess, and thus its density deficiency, relative to the environment could be calculated. In the case of August 14, the motion pictures seemed to indicate that the large bubbles were forming at about 1300 m, at which height a visible transition from main cloud body to "turret" appeared to take place, thus indicating the tectonic limit. Figure 5 is traced from the film viewer at the frame corresponding to observation 2 in Table I, and shows this division. Figure 6 shows the buoyancy calculation, the solid curve (calculated from the sounding) giving the virtual temperature curve of the environment; the dashed curve gives the virtual temperature of the bubble, calculated from the moist adiabat intersecting the sounding at 1300 m.

Table I. Bubble of August 14, 1950. Nantucket, U.S.A.
Height range studied 2200-2600 m
Cloud base 450 m; $gB = 8.2$ cm/sec^2 = constant

Observation Number	$-t$ sec	$(-t)^{\frac{1}{2}}$ sec$^{\frac{1}{2}}$	w cm/sec	$\dot{w}$ cm/sec^2	$\dot{w}/gB$	G sec$^{-\frac{1}{2}}$	R_{calc} m	w_o cm/sec	$\frac{w-w_o}{w_o}$	$(1-\dot{w}/gB)^{\frac{1}{2}} -1$
1	108	10.4	428	- 0.82	- .091	0.21	445	400	.07	.05
2*	96	9.8	410	- 0.82	- .091	0.20	390	380	.08	.05
3	84	9.2	395	- 0.98	- .119	0.20	345	352	.12	.06
4	72	8.5	378	- 1.15	- .140	0.20	295	326	.16	.07
5	60	7.8	355	- 1.30	- .159	0.19	245	300	.18	.08
6	48	6.9	326	- 1.64	- .200	0.19	195	268	.22	.09
7	36	6.0	306	- 2.80	- .342	0.19	150	232	.32	.16
8	24	4.9	276	- 5.43	- .661	0.19	100	187	.47	.29
9	12	3.5	197	-11.80	-1.44	0.23	50	133	.48	.57

$\bar{G} = 0.200$
$\delta = 15\%$
$\Delta = 20\%$

*Diameter of bubble measured on film at this frame to be 425 m

The virtual temperature difference in the observed height range is about $2.3^{\circ}C$, and nearly constant, giving the value of gB = 8.2 used in the table.

The value of $\overline{G}$ = 0.200 is the average for this bubble (coincidentally, it is nearly exactly the same as the over-all average for all eleven studied). This gives a value of E of the erosion constant of approximately 50 seconds. The variations in G within the single bubble are expressed by δ and $\triangle$, the former being the percentage maximum departure from the average, and the latter the maximum range in G divided by the average. The values of the buoyancy are probably not accurate to better than 15% thus variations that large in G may be expected due to this cause alone. Thus the value of E should be written as 50 $\pm$ $\sim$ 8 sec and is only reliable to one significant figure.

Now the last four columns in the table may be discussed. In order to test the internal consistency of the bubble model, and especially the assumption that w did not greatly exceed w_0, R may be calculated from (9) using E = 50 seconds. The limiting velocity, w_0, is then calculated from (4) using this value of R. The actual w is seen always slightly to exceed this calculated w_0. The fraction by which w exceeds w_0 is calculated in the next-to-last column. It is possible to make an independent check computation of this fraction by solving (6) for w, and subtracting v_0 from the numerator and dividing by it, giving after substitution of (4)

$$\frac{w - w_0}{w_0} = (1 - \dot{w}/gB)^{\frac{1}{2}} - 1 \tag{20}$$

The last column shows the fractional departure of w from w_0 found using this method. Since a 1 mps error in measuring w may give an error in this quantity

of 100-200%, the agreement between the two methods may be considered very
satisfactory. The angular half-aperture of the bubble may be calculated
from the relation (see Fig. 19)

$$\sin \theta_m = \frac{D}{2R} \tag{21}$$

using the measured value of D at the second observation and the corresponding
R, the angle θ_m comes out $33°$, which is on the small end of the range studied
by Davies and Taylor (1950).

Next, several trade cumulus bubbles are considered.

b. Case of June 30, 1952. St. Croix, V. I.

The largest bubble, which was also the bubble which penetrated to great-
est altitude, was photographed on this day from the island of St. Croix.
Although the films lacked sufficient contrast for reproduction, one of the
frames is traced in Figure 7, which shows the dimensions and appearance of
the bubble studied. This case was particularly important because it was the
only one permitting a direct check of the erosion law. The same calculations
as made for the preceding bubble are presented in Table II. The frames were
six seconds apart and measurements were made every fourth frame. The buoy-
ancy calculation is shown in Figure 8. On this occasion, not only did the
films indicate that the large bubbles were forming at about 1800 m, but the
sounding showed that the external lapse rate exceeded moist adiabatic up to
that level, above which it became equal to moist adiabatic, thus clearly
demarking the tectonic limit.

The value of $\bar{G}$ is seen to be nearly identical to that for the Nantucket

Table II. Bubble of June 30, 1952. St. Croix, V. I.
Height range studied 2900-4950 m
Cloud base 590 m; gB = 10.0 cm/sec² ≅ constant

Observation Number	$-t$ sec	$(-t)^{\frac{1}{2}}$ sec$^{\frac{1}{2}}$	w cm/sec	$\dot{w}$ cm/sec²	$\dot{w}/gB$	G sec^{-1}	B_{calc} m	w_o cm/sec	$\dfrac{w-w_o}{w_o}$	$(1-\dot{w}/gB)^{\frac{1}{2}}-1$
1	297	17.2	860	-0.38	-.038	0.20	1500	820	.05	.02
2	273	16.6	846	-0.63	-.063	0.20	1380	785	.08	.03
3	249	15.8	846	-0.87	-.087	0.20	1260	750	.13	.05
4	225	15.0	830	-1.20	-.120	0.19	1135	710	.17	.06
5	201	14.2	795	-1.64	-.164	0.19	1015	670	.19	.08
6	177	13.3	755	-2.08	-.208	0.19	895	635	?.19	.10
7	153	12.4	710	-2.52	-.252	0.20	770	585	.21	.12
8*	129	11.3	634	-2.96	-.296	0.20	650	540	.17	.14
9	105	10.3	550	-3.34	-.334	0.22	530	485	.13	.15
10	81	9.0	483	-3.53	-.353	0.22	410	428	.13	.16
11	57	7.5	400	-3.93	-.393	0.22	285	358	.12	.18
12	33	5.7	320	-4.72	-.472	0.22	165	273	.17	.21
13	9	3.0	196	-6.30	-.630	0.20	45	111	.39	.28

$\bar{G} = 0.204$ $\delta = 10\%$ $\Delta = 15\%$

*Diameter measured as 750 m

cloud previously studied, despite an entirely different air mass and location. The variations during the bubble's life are smaller than previously and do not exceed the error of the observations.

This bubble was so isolated on the film and maintained such a smooth spherical cap that it was possible to measure the cap diameter with some confidence from $t = -183$ sec to $t = -33$ sec. The results are plotted in Figure 9. A straight line was fitted to these points which had a slope $\triangle D/\triangle t = -4 \times 10^2$ cm/sec. Since the diameter of a bubble, according to the model, should be proportional to the radius of curvature $\triangle D/\triangle t$ should equal $\triangle R/\triangle t$. When $\triangle R/\triangle t$ is calculated from (8) it comes out $\triangle R/\triangle t = -EgB = -50 \times 10 = -5 \times 10^2$ cm/sec. Thus the observed slope departs from the theoretical by only 20% (about the accuracy with which the measured values of D adhere to the straight line in Fig. 9) and we may consider that the erosion law has been directly checked, in this one case. The half-aperture θ_m was calculated for $t = -129$ secs to be $35.5°$ and since the bubble was seen to retain its shape throughout the times represented on Figure 9, it may be deduced that this angle remained very nearly constant throughout its lifetime.

c. Case of Mr 18, 1953. Anegada, B.W.I.

Two trade cumulus bubbles over the open ocean were observed from Anegada Island (120 miles east-northeast of San Juan, Puerto Rico) on March 18, 1953. As in the preceding cases, a simultaneous airplane measurement of cloud base and a temperature sounding within a few miles of the clouds were available. A sequence from the time-lapse films showing the bubbles is presented in Figure 10. The calculation of G is presented in Tables III and IV.

Table III. Bubble 1, March 18, 1953. Anegada, B.W.I.

Height range studied 1500-1780 m

Cloud base 570 m; gB $\cong$ const. = 7.6 cm/sec^2

Observation Number	$-t$ sec	$(-t)^{\frac{1}{2}}$ sec$^{\frac{1}{2}}$	w cm/sec	$\dot{w}$ cm/sec^2	$\dot{w}/gB$	$(1-\dot{w}/gB)^{\frac{1}{2}}$	G sec$^{-\frac{1}{2}}$
1	95.8	9.8	323	-0.2	- .026	1.01	0.23
2	81.4	9.0	317	-0.4	- .053	1.03	0.22
3	67.0	8.2	308	-0.6	- .079	1.04	0.21
4	52.6	7.3	292	-0.8	- .105	1.05	0.20
5*	38.2	6.2	280	-1.2	- .158	1.07	0.18
6	23.8	4.9	263	-4.1	- .540	1.24	0.18
7	9.4	3.1	175	-8.1	-1.06	1.44	0.20

*Diameter measured roughly at
this frame to be 160 m

$\overline{G}$ = 0.203
δ = 15%
Δ = 25%

Table IV. Bubble 2, March 18, 1953. Anegada, B.W.I.

Height range studied 1380-1680 m

Cloud base 570 m; $gB \approx$ const. $= 8.0$ cm/sec^2

Observation Number	$-t$ sec	$(-t)^{\frac{1}{2}}$ sec$^{\frac{1}{2}}$	w cm/sec	$\dot{w}$ cm/sec^2	$\dot{w}/gB$	$(1-\dot{w}/gB)^{\frac{1}{2}}$	G sec$^{-\frac{1}{2}}$
1*	86.4	9.3	381	− 0.6	− .075	1.04	0.20
2	72.0	8.5	367	− 0.8	− .100	1.05	0.19
3	57.6	7.6	352	− 1.2	− .150	1.07	0.19
4	43.2	6.5	336	− 2.1	− .262	1.12	0.17
5	28.8	5.4	302	− 4.1	− .513	1.23	0.18
6	14.4	3.8	205	−10.2	−1.280	1.51	0.22

*Diameter measured very roughly as ∼ 340 m

$\bar{G} = 0.191$
$\delta = 15\%$
$\Delta = 20\%$

The time interval between frames was 3.6 seconds and observations were read off every four frames or 14.4 seconds apart.

Since these two bubbles were protrusions from a larger cloud turret (see Fig. 11), the estimation of their diameters was extremely difficult. The buoyancies were arrived at by a procedure similar to that of the preceding cases, except that examination of the film suggested that these bubbles had risen from cloud base, or very nearly. Thus the moist adiabat intersecting the sounding at cloud base was used. The diagram showing the buoyancy calculation is given in Figure 12. Since the environment lapse rate was steeper than moist adiabatic on this occasion up to 1600 m, bubble agglomeration could presumably have occurred in other bubbles much above cloud base. Several clouds in the vicinity were traversed by the aircraft on this day up to 1675 m, and it will be attempted later to determine whether this was the case.

Since these bubbles were far less isolated than the preceding cases, the degree of constancy of C is extremely satisfactory.

d. Case of April 2, 1953. Anegada, B.W.I.

A rather isolated trade-wind bubble was observed from Anegada on April 2, 1953, and a sequence from the film depicting it is reproduced in Figure 13. The pertinent calculations are presented in Table V. The frame corresponding to observation 8 has been traced and is shown in Figure 14. The origin of this bubble appeared from the film to be about 1 km, although the lapse rate slightly exceeded moist adiabatic up to about 1900 m. The buoyancy calculation is shown in Figure 15. This day was an extremely marginal one for convective clouds and bubbles only feebly succeeded one

Table V. Bubble of April 2, 1953. Anegada, B.W.I.

Height range studied 1340-1920 m

Cloud base 590 m; gB = const. = 5.6

Observation Number	$-t$ sec	$(-t)^{\frac{1}{2}}$ $sec^{\frac{1}{2}}$	w cm/sec	$\dot{w}$ cm/sec^2	$\dot{w}/gB$	$(1-\dot{w}/gB)^{\frac{1}{2}}$	G $sec^{-\frac{1}{2}}$
1	187.2	13.7	370	0	0	1	0.21
2	172.8	13.2	368	-0.17	- .030	1.015	0.20
3	158.4	12.6	362	-0.34	- .061	1.03	0.20
4	144.0	12.0	352	-0.51	- .091	1.05	0.20
5	129.6	11.4	335	-0.85	- .152	1.07	0.20
6	115.2	10.7	310	-1.02	- .182	1.09	0.21
7	100.8	10.0	295	-0.97	- .173	1.08	0.20
8*	86.4	9.3	278	-0.85	- .152	1.07	0.20
9	72.0	8.5	265	-0.85	- .152	1.07	0.19
10	57.6	7.6	253	-1.02	- .182	1.09	0.18
11	43.2	6.5	220	-1.37	- .245	1.11	0.18
12	28.8	5.4	210	-2.56	- .457	1.21	0.17
13	14.4	3.8	169	-6.0	-1.07	1.44	0.18

*Diameter measured as 290 m

$\overline{G} = 0.194$
$\delta = 10\%$
$\Delta = 20\%$

another. Further cloud studies by the airplane on this day may perhaps re-
veal the reason.

e. Case of August 8, 1950. Nantucket, U.S.A.

On this day a total of ten bubbles were observed and calculations were
made on six of these. Several of the bubbles studied individually were seen
to amalgamate, and are later discussed as an aggregate or composite bubble.
A sequence from the film showing the bubbles used is presented in Figure 16.
The individual bubble computations are shown in Tables VI-XI.

As the tables show, some of these bubbles, particularly 8, were hardly
sufficiently isolated to be treated as individual bubbles. Figure 17 illus-
trates this point more clearly. Figure 18 indicates the manner in which the
buoyancies used in the tables were deduced. On this day, the appropriate
values of gB were obtained by working backward, since the approximate value
of G was known from the preceding bubbles. It was concluded that the bub-
bles constituting the clouds on August 8 had risen all the way from the
ground, or nearly from the ground, using many pieces of evidence. Among
these was the fact that bubbles appeared again and again over preferred
positions (see Malkus and Bunker, 1952, p. 11). Also the lapse rate above
cloud base was more stable than moist adiabatic; thus the tectonic limit
must have been at cloud base (800 m). Therefore the bubbles were assumed
to have risen dry adiabatically up to cloud base and from thence moist
adiabatically, the moist adiabat being chosen in such a way as to give G
somewhere in the previously determined range. It is interesting to note
that the maximum temperature required by a bubble leaving the ground (num-
bers 9 and 10) only exceeds the observed maximum temperature at Nantucket

- 30 -

Table VI. Bubble 4, August 8, 1950. Nantucket, U.S.A.

Height range studied 1120-1320 m

Cloud base 800 m

Observation	-t	$(-t)^{\frac{1}{2}}$	w	$\dot{w}$	gB	$\dot{w}/gB$	$(1-\dot{w}/gB)^{\frac{1}{2}}$	G
Number	sec	$sec^{\frac{1}{2}}$	cm/sec	cm/sec^2	cm/sec^2			$sec^{-\frac{1}{2}}$
1	87	9.3	330	0	7.0	0	1.00	0.20
2*	72	8.5	330	-1.7	6.5	-0.26	1.12	0.19
3	57	7.6	300	-3.3	6.0	-0.55	1.25	0.19
4	42	6.5	230	-4.1	5.5	-0.74	1.32	0.20
5	27	5.2	170	-4.6	5.0	-0.92	1.39	0.21
6	12	3.5	90	-4.9	4.5	-1.09	1.44	0.25

*Diameter measured as 250 m

$\bar{G} = 0.210$
$\delta = 19\%$
$\Delta = 29\%$

Table VII. Bubble 5, August 8, 1950. Nantucket, U.S.A.

Height range studied 1250-1400 m

Cloud base 800 m

Observation Number	$-t$	$(-t)^{\frac{1}{2}}$	w	$\dot{w}$	gB	$\dot{w}/gB$	$(1-\dot{w}/gB)^{\frac{1}{2}}$	G
	sec	$\sec^{\frac{1}{2}}$	cm/sec	cm/sec^2	cm/sec^2			$\sec^{-\frac{1}{2}}$
1	60	7.7	436	0	11.0	0	1.00	0.20
2*	51	7.2	428	- 1.9	10.5	-0.18	1.09	0.19
3	42	6.5	384	- 3.3	10.0	-0.33	1.15	0.20
4	33	5.8	356	- 4.8	9.5	-0.50	1.22	0.19
5	24	4.9	296	- 6.8	9.0	-0.75	1.32	0.20
6	15	3.9	227	- 9.7	8.5	-1.14	1.46	0.21
7	6	2.5	139	-15.5	8.0	-1.94	1.72	0.25

*Diameter measured as 250 m

$\bar{G} = 0.210$
$\delta = 19\%$
$\Delta = 29\%$

Table VIII. Bubble 7, August 8, 1950. Nantucket, U.S.A.

Height range studied 1400-1670 m

Cloud base 800 m; $gB \cong$ const. $= 7.0$ cm/sec^2

Observation Number	$-t$ sec	$(-t)^{\frac{1}{2}}$ sec$^{\frac{1}{2}}$	w cm/sec	$\dot{w}$ cm/sec^2	$\dot{w}/gB$	$(1-\dot{w}/gB)^{\frac{1}{2}}$	G sec$^{-\frac{1}{2}}$
1	105	10.3	346	0	0	0	0.21
2	90	9.5	340	- 0.7	-0.1	1.05	0.20
3*	75	8.7	330	- 1.4	-0.2	1.10	0.20
4	60	7.8	314	- 2.1	-0.3	1.14	0.21
5	45	6.7	288	- 2.8	-0.4	1.18	0.20
6	30	5.5	251	- 4.2	-0.6	1.27	0.20
7	15	3.9	145	-11.2	-1.6	1.62	0.30

*Diameter too difficult to measure from film

$\overline{G} = 0.218$
$\delta = 36\%$
$\Delta = 45\%$

Table IX. Bubble 8, August 8, 1950. Nantucket, U.S.A.

Height range studied 1550-1750 m

Cloud base 800 m

Observation Number	$-t$ sec	$(-t)^{\frac{1}{2}}$ sec$^{\frac{1}{2}}$	w cm/sec	$\dot{w}$ cm/sec^2	$\dot{w}/gB$	$(1-\dot{w}/gB)^{\frac{1}{2}}$	G sec$^{-\frac{1}{2}}$
1	90	9.5	261	-1.9	-0.27	1.13	0.29
2	81	9.0	261	+1.9	+0.27	0.86	0.21
3*	72	8.5	279	+1.9	+0.27	0.86	0.18
4	63	7.9	296	+1.9	+0.27	0.86	0.16
5	54	7.3	296	+1.9	+0.27	0.86	0.15
6	45	6.7	279	0	0	1.00	0.17
7	36	6.0	261	-1.9	-0.27	1.13	0.18
8	27	5.2	220	-3.8	-0.54	1.24	0.20
9	18	4.2	192	-5.7	-0.82	1.35	0.21
10	9	3.0	130	-7.6	-1.08	1.44	0.23

*Diameter measured as 280 m

$\bar{G} = 0.198$
$\delta = 45\%$
$\triangle = 70\%$

Table X. Bubble 9, August 8, 1950. Nantucket, U.S.A.

Height range studied 1600-2000 m

Cloud base 800 m; $gB = 10.0$ cm/sec^2 = constant

Observation Number	$-t$ sec	$(-t)^{\frac{1}{2}}$ sec$^{\frac{1}{2}}$	w cm/sec	$\dot{w}$ cm/sec^2	$\dot{w}/gB$	$(1-\dot{w}/gB)^{\frac{1}{2}}$	G sec$^{-\frac{1}{2}}$
1	96	9.8	490	- 0.54	- .054	1.03	0.21
2	84	9.2	473	- 0.54	- .054	1.03	0.20
3	72	8.5	457	- 0.81	- .081	1.04	0.19
4*	60	7.8	440	- 1.08	- .108	1.06	0.19
5	48	6.9	424	- 1.75	- .175	1.08	0.18
6	36	6.0	408	- 3.10	- .310	1.15	0.17
7	24	4.9	359	- 5.80	- .580	1.26	0.17
8	12	3.5	244	-10.8	-1.08	1.44	0.21

*Diameter measured as 310 m

$\bar{G} = 0.190$
$\delta = 10\%$
$\Delta = 21\%$

Table XI. Bubble 10, August 8, 1950. Nantucket, U.S.A.

Height range studied 1650-2260 m

Cloud base 800 m; $gB = 10.0$ cm/sec^2 = constant

Observation Number	$-t$ sec	$(-t)^{\frac{1}{2}}$ sec$^{\frac{1}{2}}$	w cm/sec	$\dot{w}$ cm/sec^2	$\dot{w}/gB$	$(1-\dot{w}/gB)^{\frac{1}{2}}$	G sec$^{-\frac{1}{2}}$
1	117	10.6	540	-1.5	$-.15$	1.07	0.21
2	105	10.2	520	-1.6	$-.16$	1.08	0.21
3*	93	9.6	500	-1.7	$-.17$	1.08	0.21
4	81	9.0	490	-2.0	$-.20$	1.10	0.20
5	69	8.3	460	-2.4	$-.24$	1.11	0.20
6	57	7.5	420	-3.0	$-.30$	1.14	0.20
7	45	6.7	370	-3.8	$-.38$	1.18	0.21
8	33	5.7	340	-5.0	$-.50$	1.23	0.21
9	21	4.6	290	-6.7	$-.67$	1.29	0.21
10	9	3	210	-10.0	-1.0	1.42	0.20

*Diameter measured as 390 m

$\bar{\bar{G}} = 0.206$
$\delta = 5\%$
$\Delta = 5\%$

airport by $0.2^{o}C$. It is not implausible that the later bubbles should have
required warmer initial temperatures since they were observed to penetrate
to greater heights than their predecessors. It is also interesting to note
that bubbles 4 and 5 required variable buoyancy. To obtain a mean buoyancy
of the proper value to arrive at a $G \approx 0.20$, a moist adiabat had to be cho-
sen for these bubbles which gave decreasing buoyancy with height, although
the rate of decrease was within the range for which equation (11) should
apply (see pp. 11, 12 and the Appendix). When the changing values of gB
were read from the appropriate moist adiabat in Figure 18, however, Tables
VI and VII show that G still retains a satisfactorily constant value.

f. Summary of the Observations of Individual Bubbles

The average value of $\bar{G}$, called $\bar{\bar{G}}$, for all the bubbles, is just slightly
greater than $0.2 \ sec^{-\frac{1}{2}}$. Using $\bar{\bar{G}}$ in equation (11), the average value of E
comes out 54 seconds, and will henceforth be used as 50 seconds, since the
accuracy of the observations is such that only the first figure is signifi-
cant. Table XII compares all the values of $\bar{G}$. The greatest departure, δ ,
from the average is 8% and the total spread from minimum to maximum divided
by the average, $\triangle$, is 15%, which is within the accuracy of the measure-
ments. The fluctuations of G obtained within the life of a single bubble
can, where they occur, nearly always be accounted for by the interference
of another bubble or a wake, which usually caused the measured velocities
to be too high.

The average angular half-aperture θ_m of the bubbles may be estimated
by comparing the measured values of the bubble diameter D, obtained for the
starred observation in each table, and the radius of curvature, R, calculated

Table XII. Radius and w_o calculation for each bubble at time $(-t)^*$ and comparison of values of $\bar{G}$

Bubble Date and Number	Time $(-t)^*$ sec	D measured meters	R calc. from E meters	w_o calc. cm/sec	$\dfrac{w-w_o}{w_o}$ at $(-t)^*$	$(1-\dot{w}/gB)^{\frac{1}{2}}$ -1 at $(-t)^*$	$\bar{G}$ sec$^{-\frac{1}{2}}$
Aug. 14	96	425	390	380	.08	.05	0.200
June 30	129	750	650	540	.17	.14	0.204
#1, March 18	382	160	145	220	.27	.07	0.203
#2, March 18	86.4	340*	345	350	.09	.04	0.191
April 2	86.4	290	240	250	.11	.07	0.194
#4, Aug. 8	72	250	230	260	.27	.12	0.210
#5, Aug. 8	51	250	270	355	.20	.09	0.210
#7, Aug. 8	75	too diff- cult to measure	260	285	.16	.10	0.218
#8, Aug. 8	72	280	250	280	0	-.14	0.198
#9, Aug. 8	60	310	300	370	.19	.06	0.190
#10, Aug. 8	93	390	465	455	.10	.08	0.206

*Very rough measurement

$\bar{\bar{G}} = .202$
$\cong 0.2$
$\delta = 8\%$
$\Delta = 15\%$

from equation (9), $R = -EgBt$. Using E equal to 50 seconds the corresponding values of R are given in the fourth column from the left in Table XII. The average ratio D/R is approximately one, giving an average θ_m of 30°, as illustrated in Figure 19. The few cases where it was possible to measure D fairly accurately (August 14 and June 30) indicate that θ_m probably should be a few degrees larger than this. The next column in Table XII gives at $(-t)^*$ calculated using the values of R in equation (4). The fractional departure of the measured w at $(-t)^*$ from w_0 is also given in the table and should be equal to $(1 - \dot{w}/gB)^{\frac{1}{2}} - 1$ which is presented beside it (see equation (20), p. 21). Although the departures between these two sets of results are within observational error, it will be noted that the one calculated from accelerations is systematically smaller than the other. This may perhaps be an indication that a factor greater than one should have been multiplied by the inertial term in equation (6). It may only indicate that the method of measuring $\dot{w}$ from the films using smoothed second differences in heights gives results which are systematically too small. There is no apparent theoretical way of arriving at any factor greater than one to be multiplied by the inertial term in equation (6) and even if there were, no way exists at present of testing it observationally. Therefore nothing will be done here to complicate the model, which has worked out quite satisfactorily.

Thus it may be concluded that for relatively isolated cloud bubbles the proposed force and erosion laws are applicable. The importance of this conclusion lies in the simplicity of the laws and the independence of the bubble's life cycle from government by vast numbers of environment parameters.

In order to progress from a single bubble to a cumulus, however, we must consider the interaction of many bubbles with one another and with their environment, and we must eventually attempt to study the process of wake formation. As a first step in the direction of this building process, the interaction of several bubbles to produce a larger one may be considered, since information on this point is at present available.

IV. THE INTERACTION OF BUBBLES WITH ONE ANOTHER AND WITH THE ENVIRONMENT

In Tables I-XI, bubbles ranging in diameter from about 100 m to about 1 km were studied. Some of the larger ones were visibly composed of bubbles of a smaller size which often made themselves apparent as the bumpy nodules at the top. Concerning the origin of the smaller bubbles ($\sim$ 100 m) several mechanisms immediately suggest themselves. One is irregularities in surface heating or "hot spots" on the ground, as were probably witnessed in the Nantucket case of August 8. In the case of trade cumulus, small bubbles may originate at cloud base when some of the eddies in the mixed subcloud layer (50-150 m diameter) strike their condensation level. It is interesting to note that none of the trade cumulus bubbles studied here appeared to originate below cloud base.

Concerning the aggregation of these small bubbles into tower-sized larger ones, some light is shed by the fundamental work on a convecting fluid. In considering such a medium, W. Malkus (1953) showed that the fluid as a whole and the individual elements therein will organize in such a manner as to maximize the potential energy dissipation into other forms. In the case of rising bubbles, this dissipation is maximized if the product gBw is maximized. Equation (4) shows that larger bubbles will possess a

higher ascent velocity. Thus the larger elements will be preferred. It is not yet clear what places an upper limit upon the size which may be achieved by aggregation, although this is probably related to the vertical dimensions of the convecting fluid layers.

a. A Case of the Aggregation of Several Small Bubbles into a Larger Composite Bubble

On August 8, 1950, the amalgamation process took place before the eyes of the observers, bubbles 5, 6, and 7 joining together to constitute the large tower dominating the middle column of photographs in Figure 16. The composite bubble is shown in Figures 17b and 17c, which illustrate how the smaller, numbered bubbles continued to be identified as protrusions from the top of this composite bubble, exhausting at different levels as they each execute their own life cycle. Figure 20 shows the height-time curve for each of these individuals and the composite formed by them. The resulting calculation for the composite bubble is presented in Table XIII.

The buoyancy for the composite bubble was determined merely by taking that constant value of gB which gave G in the range obtained for the other bubbles studied. The value of gB = 4.5 implies a virtual temperature excess of the bubble of 1.3°C, or since the bubble is ascending moist adiabatically, an actual temperature difference of 1.0°C and an increment due to excess water vapor of 0.3°C. These values were obtained from the thermodynamic diagram assuming that the composite bubble was formed at cloud base (tectonic limit for this day) and from there followed up a wet adiabat. Its excess virtual temperature of 1.3°C at this level is to be compared to excesses of about 3.6°C for the corresponding individual bubbles. Unfortunately, during the latter part of its history (from -t = 120 sec onward)

Table XIII. Composite bubble of August 8, 1950. Nantucket, U.S.A.

consisting of individuals 5, 6, and 7

Height range studied 1090-1730 m

Cloud base 600 m; $gB = 4.5$ cm/sec^2 = constant

Observation Number	$-t$ sec	$(-t)^{\frac{1}{2}}$ sec$^{\frac{1}{2}}$	w cm/sec	$\dot{w}$ cm/sec^2	$\dot{w}/gB$	$(1-\dot{w}/gB)^{\frac{1}{2}}$	G sec$^{-\frac{1}{2}}$
1*	240	15.5	314	-0.28	-.062	1.03	0.23
2	225	15.0	304	-0.28	-.062	1.03	0.23
3	210	14.5	304	-0.28	-.062	1.03	0.22
4	195	14.0	304	-0.28	-.062	1.03	0.21
5	180	13.5	294	-0.28	-.062	1.03	0.21
6	165	12.8	294	-0.28	-.062	1.03	0.20
7	150	12.2	282	-0.28	-.062	1.03	0.20
8	135	11.6	282	-0.28	-.062	1.03	0.19
9	120	11.0	272	-0.28	-.062	1.03	0.19
10	105	10.3	272	-0.28	-.062	1.03	0.18
11	90	9.5	262	-0.28	-.062	1.03	0.17
12	75	8.7	248	-0.35	-.078	1.04	0.16
13	60	7.8	238	-0.49	-.109	1.06	0.16
14	45	6.7	228	-1.75	-.390	1.18	0.16
15	30	5.5	198	-3.08	-.685	1.30	0.16
16	15	3.8	126	-4.90	-1.09	1.45	0.20

*Diameter measured as 500 m

$\bar{G} = 0.192$
$\delta = 21\%$
$\Delta = 37\%$

the composite bubble was being followed closely and pushed upward by bubble 8 (see Fig. 17c) and thus the vertical motions measured are too high, giving excessively low values of G in Table XIII. Nevertheless, it may be considered to obey the laws for a single bubble fairly well, as is supported by the calculation of R from equation (9). At $-t = 240$ seconds, using E = 50 seconds, R comes out 540 m, giving an angular half-aperture, θ_m, of about 28°. From (4), using the calculated R, w_o comes out 325 cm/sec which is within observational error of the measured w.

Certain other deductions concerning the composition and formation of this bubble may be drawn from Figure 20 and the tables. At $-t = 180$ seconds on the composite bubble's time scale, its top was at 1300 m. It was then composed of bubbles 5 and 6. Extrapolating with the formula $R = -EgBt$ at this frame the composite bubble would have a radius of curvature equal to about 400 m, while bubble 5 would have dwindled to about 100 m and bubble 6 to about 300 m. Assuming the volume proportional to the cube of this linear dimension, it may be hazarded that approximately 30% of the large bubble volume came from undilute individuals and 70% from wake material. No inferences are drawn about the degree of mixing or homogeneity within the large bubble, which must however be fairly high for it to retain coherent identity. If the individual bubbles possessed, at the time, a buoyancy gB of 10.0 cm/sec^2 and the composite bubble a gB of 4.5 cm/sec^2, this means the wake material had buoyancy of roughly gB = 2.0 cm/sec^2. This would imply a virtual temperature excess in the wake of 0.58°C. Using the entrainment method of Stommel (1947) it is possible to determine what degree of mixing between cloudy air and environment would give rise to this latter buoyancy at this height. When the virtual temperature excess

- 43 -

possessed by bubble 5 at cloud base was assumed to derive initial values of temperature and moisture, the entrainment rate between cloud base and 1200 m averaged about 1.5×10^{-5} cm^{-1}. This is in good agreement with the entrainment rate (2.0×10^{-5} cm^{-1}) calculated by Malkus (1952b) for the same clouds using their observed slopes.

b. Interaction between Bubbles and Their Environment

Most of the important recent work on cumulus clouds has emphasized the critical role of the ambient air in regulating the formation, growth, and development of the clouds. In particular, it has been shown (Austin, 1948; Byers and Braham, 1949; Byers and Battan, 1949; Malkus, 1952a) that strong wind shear and environment dryness are inhibitory to the growth of large clouds and precipitation. The present study has so far dealt with individual bubbles whose life history in relative isolation has been shown to be rather unaffected by the latter parameters, (see Appendix II for evaluation of the effects of wind shear upon a single bubble). Nevertheless, in the course of this work certain information has been derived which may provide a start on the vital problem of the protection of bubbles by one another and their interaction with the surroundings.

In particular, the level of bubble origin has been deduced in each case. This origin is usually well within the cloud body, and thus the total height range traversed by a bubble is usually far in excess of the height range studied here. The height range studied here, noted in the heading of each table, is always that following the emergence of the bubble from the cloud top when the bubble is travelling unprotected by others against erosion. Thus we are in a position to compare the total height range traversed by a

- 44 -

bubble, the relative portion of this during which it has been protected by others, its maximum radius, and environment parameters such as dryness and wind shear. This comparison is made in Table XIV. By the maximum radius of a bubble is meant the radius it had when it first emerged from the cloud top into clear air (i.e. first observed on the film). This was calculated from R at the starred frame, called R^*, by the relation $R_{max} = R^* (-t)_{max}/(-t)^*$ where $(-t)_{max}$ is the first value of $(-t)$ used in the table for each bubble. The Δq, or moisture deficiency of the environment air relative to cloudy air was deduced by subtracting the mean mixing ratio of the environment in the cloud layer from the mean mixing ratio of the appropriate bubble ascent curve. The cloud width was determined from the films, using in each case the cloud body from which the particular bubble appeared.

In the table, the protected height range was deduced by subtracting the height range studied (the unprotected height range) from the total height range, which is the difference between the topmost height penetrated by the bubble while still active, and its hypothesized level of origin. The protected height range is straightforward in all cases except August 8, since on the other days it denotes travel of the bubbles within visible cloud. On August 8, the protected height range implicitly includes the 800 m clear ascent from ground to cloud base, and the degree to which the bubbles were protected by neighbors from erosion in this range is unknown.

With these and other reservations, however, some interesting suggestions may be drawn from the table. The first is the near equality of the maximum radius of the bubble at emergence from cloud top and its length of

Table XIV. Bubble height ranges compared to environment parameters

Date	Bubble number	R_t Total Height Range meters	R_p Protected Height Range meters	R_u Unprotected Height Range meters	R_{max} Max. Radius meters	Cloud Width meters	$\dfrac{R_{max}}{R_t}$	$\dfrac{R_t}{R_{max}}$	$|b|$ Abs. value of external shear mps/Km	Moisture defic. Δq gm/Kgm	$|b|\,\Delta q$ mps/Km x gm/Kgm
Aug. 8	4	0-1320	1120	200	280	400	1.4	4.7	1.9	4.0	7.6
"	5	0-1400	1200	150	320	800	2.1	4.4	1.9	4.0	7.6
"	7	0-1670	1400	270	365	800	1.3	4.6	1.9	4.0	7.6
"	8	0-1750	1550	200	315	800	1.6	5.5	1.9	4.0	7.6
"	9	0-2000	1600	400	480	1400	1.2	4.2	1.9	4.0	7.6
"	10	0-2260	1650	610	585	1400	1.0	3.9	1.9	4.0	7.6
"	Comp.	800-1730	290	640	540	800	0.8	1.7	1.9	4.0	7.6
Aug. 14	only	1300-2600	900	400	440	2000	1.1	2.9	5.0	4.0	20.0
Mar. 18	1	580-1780	920	280	360	1000	1.3	3.3	3.0	2.7	8.0
"	2	580-1680	800	300	345	1000	1.2	3.2	3.0	2.7	8.0
Apr. 2	only	1000-1920	340	580	525	1000	0.9	1.7	3	4.6	13.8
June 30	only	1830-4950	1070	2050	1500	4000	0.7	2.1	2.2	7.1	15.6
							Ave. 1.2				

unprotected rise therefrom. The maximum radius is, on the average, about 20% larger than the height interval covered during the erosion period. On the other hand, the width of the cloud body from which the bubbles emerge seems to be very comparable, except in the case of August 8, to the total height range covered by the bubbles, as predicted by Ludlam and Scorer (1953).

Also of interest is a comparison in each case between the protected and unprotected height ranges. Except in the cases of the large composite bubbles (of 8 August and 30 June) the good days for convection seem to be characterized by large protected ranges compared to the unprotected, while poor days for convection, notably April 2, showed the reverse. Good days for convection were apparently also indicated by large values of the ratio total height range divided by maximum radius, which is given in the fourth column from the right. This is, again, essentially a measure of how large a fraction of its height range a bubble is protected by neighbors and wakes, since we have shown that once they become isolated all bubbles obey the same erosion laws. It was desired to determine what relation, if any, this ratio bore to the significant environment parameters, wind shear and moisture deficiency. To make a rough estimate of such a relation, these environment parameters were multiplied together and their product (given in the right-hand column of the table) correlated with the ratio R_t/R_{max}. The correlation coefficient came out -0.7. With this many pairs, random numbers would produce a correlation this high once in one hundred times. Although this simple correlation may or may not be physically meaningful, these data suggest a negative relation between protected height range and

environment shear and dryness, and a positive relation between good cumulus building and a high value of protected height range. Although the remarks made concerning this table are not supported by sufficient evidence to be more than very tentatively put forward, the next steps in cumulus work probably must consider relations such as these more intensively.

V. CONCLUDING REMARKS: COMPARISON BETWEEN THE PRESENT RESULTS AND PREVIOUS WORK ON CUMULUS CLOUD DYNAMICS

The critically time-dependent nature of the size and velocity of an individual convective element has been emphasized in this work. In fact, referring again to equation (11), we can see that the vertical velocity w obeys a $(-t)^{\frac{1}{2}}$ power law throughout a large portion of the bubble's life cycle. Since Q has been established constant, this law will be obeyed very accurately when the buoyancy gB is constant, up until the time near the end of the cycle when $\dot{w}$ becomes comparable to gB in magnitude. Furthermore, it has been shown that the life cycle of the isolated bubble, once formed, is independent of all environment parameters except lapse rate.

These results might at first glance appear in distinct contradiction to the basic hypothesis of the entrainment model of a cumulus evolved by Stommel (1947; 1951), Malkus (1949; 1952a, b; 1953) and others, which treats a cloud as consisting of steady or quasi-steady columnar updrafts and strongly emphasizes the effects of the environment upon the cloud. The apparent contradiction is only superficial, however, and the present work may be considered as the next logical step forward from the entrainment model, since it attempts to describe the mechanism of the entrainment, the interaction of cloud elements with one another and with the environment, and begins to

introduce some time-dependent features, at least with respect to individual cloud turrets. The necessity to progress to a time-dependent model has been long felt by workers in this field (Malkus, 1952a; 1953) and its commencement herein sheds considerable light retroactively upon the results obtained by use of the steady-state hypothesis. Indeed, the present work raises the question of how was it possible that the model of entrainment in a steady-state updraft compared so very well with the features of observed clouds, most notably in the cases described by Malkus (1953). The answer to this question should provide some clues concerning how large clouds are built up.

It should be recalled that most of the testing of the steady-state model has been carried out in the trade-wind region where clouds of 1-1.5 km vertical extent have been observed remaining in apparently steady conditions for well over one hour, sometimes longer. It must also be emphasized that during the latter study only those clouds were picked for measurement which appeared to be in this condition and data were not used for those clouds in which this proved not to be the case. The fact that so much selection had to be applied in obtaining cases to test the theory clearly indicated that at any given instant the clouds chosen were atypical of the cloud population, although it was assumed that a large fraction of this population went through a quasi-steady phase of their life cycle. Furthermore, near the tops and tower portions of these clouds the steady-state model began to give less consistent and satisfactory results, although it checked excellently in the lowest two-thirds of the cloud body.

It can now be seen that in order for the main body of a cumulus to maintain itself in a nearly steady condition, i.e. so that a set of airplane

- 49 -

traverses made through it at one instant could be similar to another set 15 minutes or so later, bubbles must be forming within and rising through it in fairly rapid succession. Also the individual bubbles which agglomerate to form the large turrets must be small compared to the size of the cloud, otherwise the character of the drafts as measured would be greatly altered by the passage of one bubble. Since the observed draft diameters in trade-wind clouds were about 1 km and the turrets from 1-1.5 km diameter, they could indeed be considered large with respect to 200-300 m bubbles.

In conclusion, although one of the aims of the bubble model may eventually be the building up of such large, quasi-steady clouds, there are many intervening steps which, at least, are now suggested by comparison of the results of the two approaches. The first of the steps should probably concern the process of wake formation by a single bubble and the effect upon a succeeding bubble of rising in this wake.

Acknowledgments

Appendix I

Consideration of More General Erosion Laws

Starting from the differential equation

$$\frac{dw}{dt} + \frac{9}{4R}w^2 = gB \qquad (6)$$

it would be extremely desirable to eliminate R, a function of time, without making an assumption concerning the exact nature of the erosion law or the constancy of the buoyancy, gB. This is feasible if we introduce equation (8) as a definition, namely

$$\frac{dR}{dt} = - EgB \qquad (8)$$

in which E may still depend upon t, w, gB or any other parameters and gB may vary in an arbitrary manner with time. The bubble's radius of curvature is eliminated between (8) and (6) by solving (6) for R, differentiating with respect to time and equating the expression for $dR/dt \equiv \dot{R}$ to -EgB. When the result is solved for G, the equation analogous to (11) is

$$\frac{3}{2} E^{-\frac{1}{2}} \equiv G = \frac{\left[1 - \dot{w}/gB\right]^{\frac{1}{2}} gB}{\left[- 2w\dot{w} + \dfrac{gB\dot{w}^2}{gB(1 - \dot{w}/gB)} - \dfrac{\ddot{w}w^2}{gB(1 - \dot{w}/gB)}\right]^{\frac{1}{2}}} \qquad (22)$$

where each dot above a symbol indicates one differentiation with respect to time. In order more rigorously to establish the constancy of G it would of

course be desirable to use equation (22) with the observed quantities. Unfortunately, the presently available observations do not permit adequate determination of $\ddot{w}$, the time rate of change of acceleration and generally $\dot{B}$ is even more difficult to obtain.

It is possible now, however, to establish the maximum permissible time variations in B for use of equation (11). For this purpose equations (6) and (8) may be combined to give

$$\frac{3}{2} E^{-\frac{1}{2}} \equiv G = \frac{\left[1 - \dot{w}/gB\right]^{\frac{1}{2}} gB}{\left[- 2w\dot{w} + \frac{4}{9} g\dot{B}R - \frac{4}{9} R\ddot{w}\right]^{\frac{1}{2}}} \tag{23}$$

where R has not been totally eliminated. First, large bubbles of about 1 km radius of curvature and approximately 10 mps ascent rates are considered. Under these conditions if B changes by 1/3 in 100 seconds, the most unfavorable combination of $\dot{w}$ and $\ddot{w}$ which might be expected gives a $\dot{B}$ term whose omission produces a 20% error in G. For smaller bubbles, the error may be shown to be considerably less for the same variation in B and any plausible combination of the other parameters. At the present stage of the work, therefore, it is quite adequate to use equation (11) provided that variations in B do not exceed about 30% in 100 seconds.

An erosion law considerably less general than one allowing E to depend in any manner on any number of arbitrary parameters is

$$\frac{dR^3}{dt} = - 3E \, (gB)^m \, w^{2n} \, R^2 \tag{24}$$

or

$$\frac{dR}{dt} = - E\,(gB)^m\,w^{2n} \qquad (24a)$$

where E is now assumed constant and m and n are to be determined.

Since $w \approx w_0$, we may write approximately

$$\frac{dR}{dt} = - E\,(gB)^{m+n}\left(\frac{2}{3}\right)^{2n} R^n \qquad (25)$$

Therefore

$$R = \left[-(1-n)\left(\frac{2}{3}\right)^{2n}(gB)^{m+n} Et \right]^{\frac{1}{1-n}} \qquad (26)$$

if $t = 0$ at $R = 0$.

Thus introducing (26) into the differential equation (6) we have

$$\frac{9}{4}\left[\left(\frac{3}{2}\right)^{2n}\frac{E^{-1}}{1-n}\right]^{\frac{1}{1-n}} = \frac{(gB - \dot{w})\,gB^{\frac{m+n}{1-n}}(-t)^{\frac{1}{1-n}}}{w^2} \qquad (27)$$

The left-hand side of (27) is a constant. If we choose a bubble for which B is constant and in the part of its life cycle where $\dot{w} \ll gB$, then, the equation

$$w^2 = \text{constant} \cdot (-t)^{\frac{1}{1-n}} \qquad (28)$$

will determine n.

From the observations we find that $n = 0$ gives the best fit. This means

the bucyancy is the chief cause of the erosion, as expected. It also means that no approximation is necessary in order to obtain (25) from (24a). Thus (27) becomes

$$\frac{9B^{-1}}{b} = \frac{(gB)^{m} (gB - \dot{w})}{w^{2}} (-t)$$

or

$$\frac{3}{2} = B^{-1} = G = \frac{gB^{\frac{m+1}{2}} (1 - \dot{w}/gB)^{\frac{1}{2}}}{w} (-t)^{\frac{1}{2}} \tag{29}$$

In the cases of those bubbles where $gB = $ constant no evaluation of m is possible. The two cases where gB varied indicate that $m = 1$ is satisfactory, although the test is not at present a rigorous one.

Appendix II

Ascent through Vertical Wind Shear

When the bubble ascends through a wind field $U(z)$ and U changes with height, the buoyant element will, in general, acquire a relative horizontal velocity, u. Under these conditions the vertical equation of motion becomes

$$\dot{w} = \frac{-w}{\sqrt{u^2 + w^2}} \; K \; (u^2 + w^2) + gB \tag{30}$$

Only drag forces operate in the horizontal, so that

$$\dot{u}_b = \frac{-u}{\sqrt{u^2 + w^2}} \; K \; (u^2 + w^2) \tag{31}$$

where u_b is the horizontal velocity of the bubble when the positive horizontal axis points in the direction of U. Then since

$$\dot{u} = \dot{u}_b - \dot{U} \tag{32}$$

$$\dot{u} = - wU' - \frac{u}{\sqrt{u^2 + w^2}} \; K \; (u^2 + w^2) \tag{33}$$

because

$$\dot{U} = wU' = w \; \frac{dU}{dz}$$

In constant wind shear at the limiting velocity of the bubble, we have

$$K \; (u_0^2 + w_0^2) = (g^2 B^2 + w_0^2 U'^2)^{\frac{1}{2}} \tag{34}$$

and analogously to equation (4)

$$\left[u_0^2 + w_0^2 \right]^{\frac{1}{2}} = \frac{2}{3} \left[(g^2 B^2 + w_0^2 U'^2)^{\frac{1}{2}} R \right]^{\frac{1}{2}} \tag{35}$$

so that

$$K = \frac{9}{4R} \tag{36}$$

as before.

This result is extremely important, for if the drag was proportional to $K (u^2 + w^2)^{n/2}$ where n now differs from 2, equation (34) becomes

$$K (u_0^2 + w_0^2)^{n/2} = g^2 B^2 + w_0^2 U'^2 \tag{37}$$

and (35) is unchanged. If we then raise (35) to the power n, we obtain, dividing it into (37)

$$K = \frac{3^n}{2^{2n}} (g^2 B^2 + w_0^2 U'^2)^{\frac{1}{2} - \frac{n}{4}} R^{-n/2} \tag{38}$$

This means that if the drag is not taken proportional to w^2, i.e. n = 2, then K has a different form when $U' \neq 0$ from that when $U' = 0$. If it is desired that K depend only upon R, then R must change in a complicated manner when the bubble ascends through shear and the bubble's shape could hardly remain similar to the normal case. The observations do not indicate these complications, thus the square-power drag law if further affirmed.

We may now deal further with equation (30) and by introducing (36) and $R = -RgBt$ obtain the analog of (11), namely

$$\frac{3}{2} E^{-\frac{2}{3}} \equiv G = \frac{gB\,(1 - \dot{w}/gB)^{\frac{1}{2}}}{\sqrt{w\,(w^2 + u^2)^{\frac{1}{2}}}} \; (-t)^{\frac{1}{2}} \qquad (39)$$

which is, strictly speaking, the equation which should be used when bubbles rise through a shearing wind field. It may be seen, however, that when $u \approx w$, the denominator of (39) is only 20% underestimated.

The order of magnitude of u will now be ascertained. We may estimate it from (33) when $\dot{u} \approx 0$. This gives

$$u = \frac{w}{(u^2 + w^2)^{\frac{1}{2}}} \frac{U'}{K} \qquad (40)$$

$$= \frac{w}{(u^2 + w^2)^{\frac{1}{2}}} \frac{4RU'}{9} \qquad (40a)$$

$$\approx \frac{4RU'}{9} \quad \text{when} \quad u^2 << w^2 \qquad (40b)$$

or, without the approximation

$$\frac{u}{w} = \frac{4RU'}{9\sqrt{u^2 + w^2}} \qquad (41)$$

The order of magnitude of u/w may be calculated roughly by putting

$$\sqrt{u^2 + w^2} \approx w_0 = 2/3\,(gBR)^{\frac{1}{2}}$$

so that

$$\frac{u}{w} \cong \frac{2R^{\frac{1}{2}} U'}{3\,(gB)^{\frac{1}{2}}} \qquad (42)$$

For the bubbles studied in this paper the highest value of the wind shear was 5×10^{-3} cm^{-1}. If R = 0.5×10^{5} cm and gB = 8 cm/sec^{2} we have u $\cong$ 0.25 w and an error in the denominator of (39) which is less than two per cent. Only in cases of bubbles 1-2 km in radius, in wind shears of 20-30 mps/km or more will u $\approx$ w and then G will be about 20% too high due to this cause.

References

Austin, J. M., 1948: A note on cumulus growth in a non-saturated environment. J. Meteor., 5: 103-107.

Byers, H. R. and L. J. Battan, 1949: Some effects of vertical wind shear on thunderstorm structure. Bull. Amer. Met. Soc., 30: 168-175.

Byers, H. R. and R. R. Braham, 1949: The Thunderstorm. Final report of the Thunderstorm Project. Washington, U. S. Gov't Printing Office: 282 pp.

Davies, R. M. and G. I. Taylor, 1950: The mechanics of large bubbles rising through extended liquids and through liquids in tubes. Proc. Roy. Soc. London, A, 200: 375-390.

Goldstein, S., 1938: Modern Developments in Fluid Dynamics. Vol. I. Oxford Univ. Press, Oxford: 330 pp.

Ince, E. L., 1944: Ordinary Differential Equations. Dover Publications, New York: 558 pp.

Ludlam, F. H. and R. S. Scorer, 1953: Reviews of modern meteorology, 10. Convection in the atmosphere. Q. J. Roy. Met. Soc., 79: 317-341.

Malkus, J. S., 1949: Effects of wind shear on some aspects of convection. Trans. Amer. Geophys. Un., 30: 19-25.

Malkus, J. S., 1952a: Recent advances in the study of convective clouds and their interaction with the environment. Tellus, 2: 71-87.

Malkus, J. S., 1952b: The slopes of cumulus clouds in relation to external wind shear. Q. J. Roy. Met. Soc., 78: 530-542.

Malkus, J. S., 1953: Some results of a trade cumulus cloud investigation. Woods Hole Oceanogr. Inst. Ref. No. 53-30. Manuscript in press, J. Meteor.

Malkus, J. S. and A. F. Bunker, 1952: Observational studies of the air flow over Nantucket Island during the summer of 1950. Pap. Phys. Oceanogr. Meteorol., Mass. Inst. of Tech. and Woods Hole Oceanogr. Inst.: 50 pp.

Malkus, J. S. and M. E. Stern, 1953: The flow of a stable atmosphere over a heated island, Part I. J. Meteor., 10: 30-41.

Rouse, Hunter, 1938: Fluid Mechanics for Hydraulic Engineers. McGraw-Hill Co., New York: 422 pp.

Scorer, R. S. and F. H. Ludlam, 1953: Bubble theory of penetrative convection. Q. J. Roy. Met. Soc., 79: 94-103.

Stommel, H., 1949: Entrainment of air into a cumulus cloud. J. Meteor., 4: 91-94.

Stommel, H., 1951: Entrainment of air into a cumulus cloud II. J. Meteor., 8: 127-129.

Sutton, O. G., 1947: The atom bomb as an experiment in convection. Weather, 2: 105-109.

Taylor, G. I., 1950: Formation of a blast wave by a very intense explosion. I. Theoretical discussion. II. The atomic explosion of 1945. Proc. Roy. Soc. London, A, 201: 159-175.
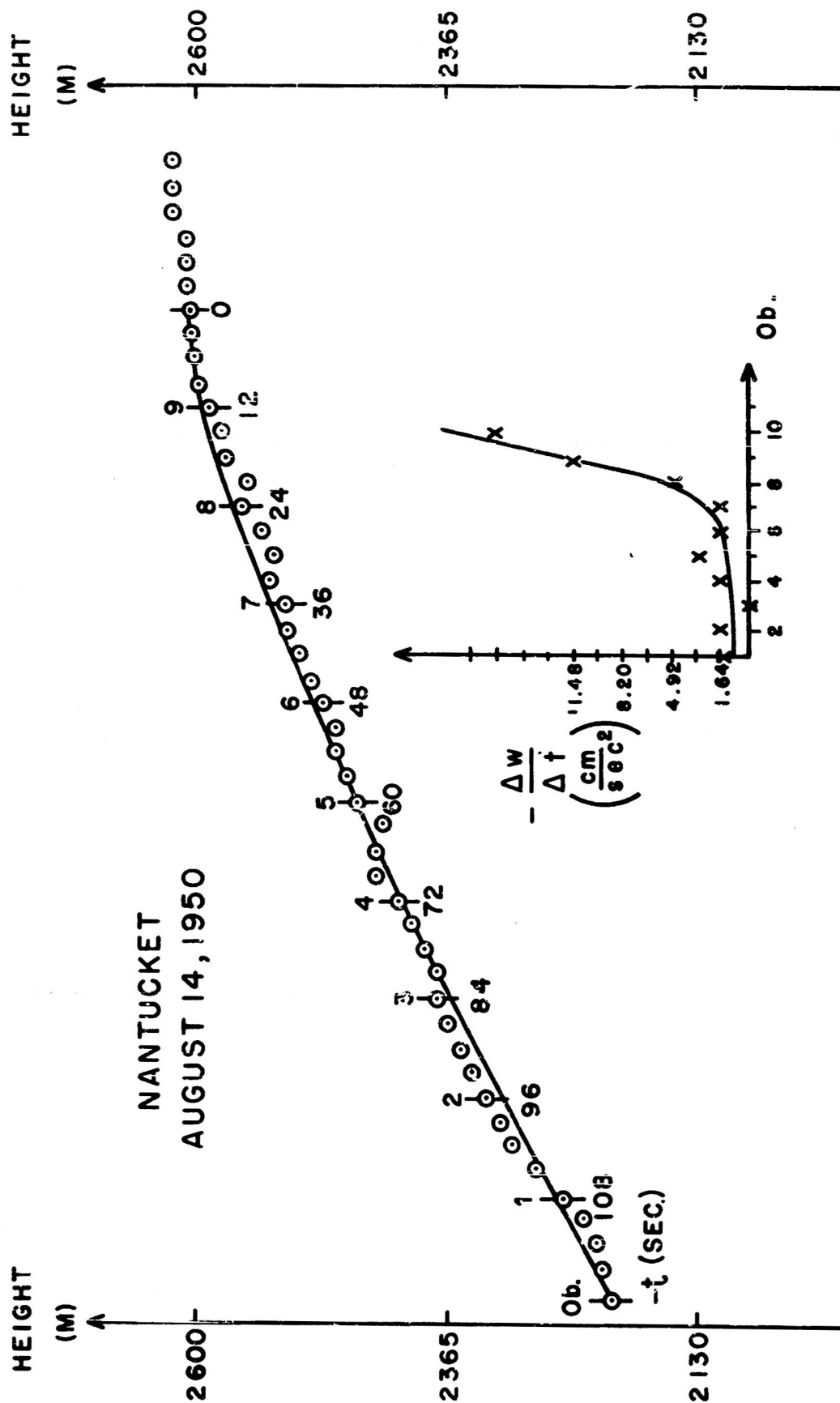
FIG.1

FIG. 2
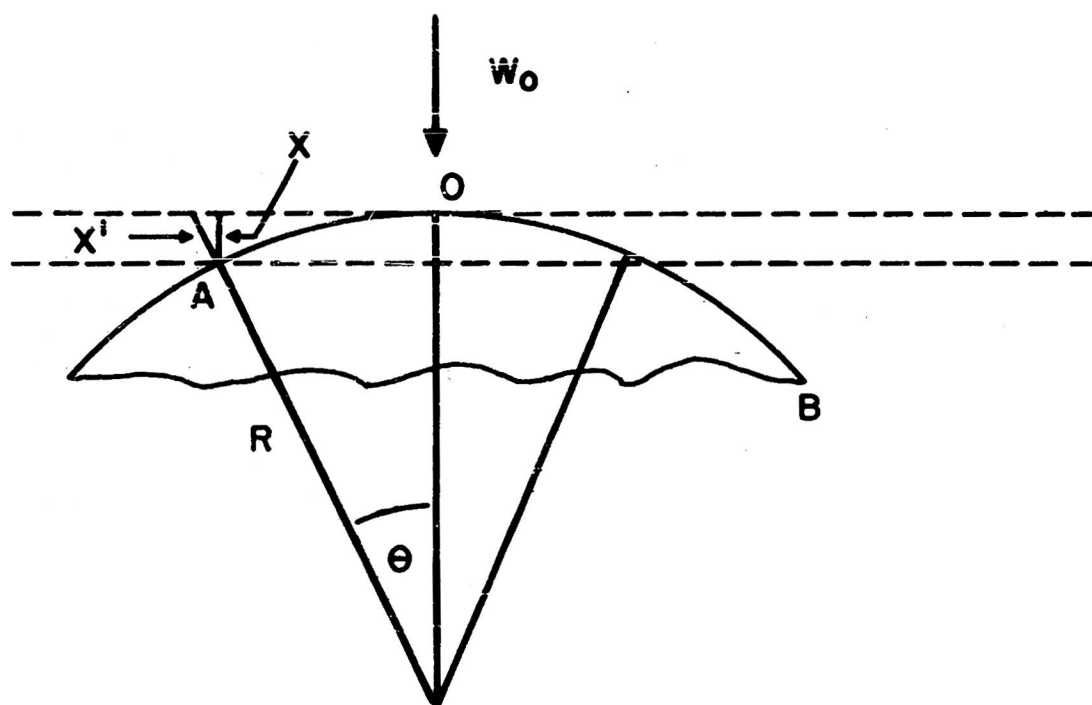
FIG. 3
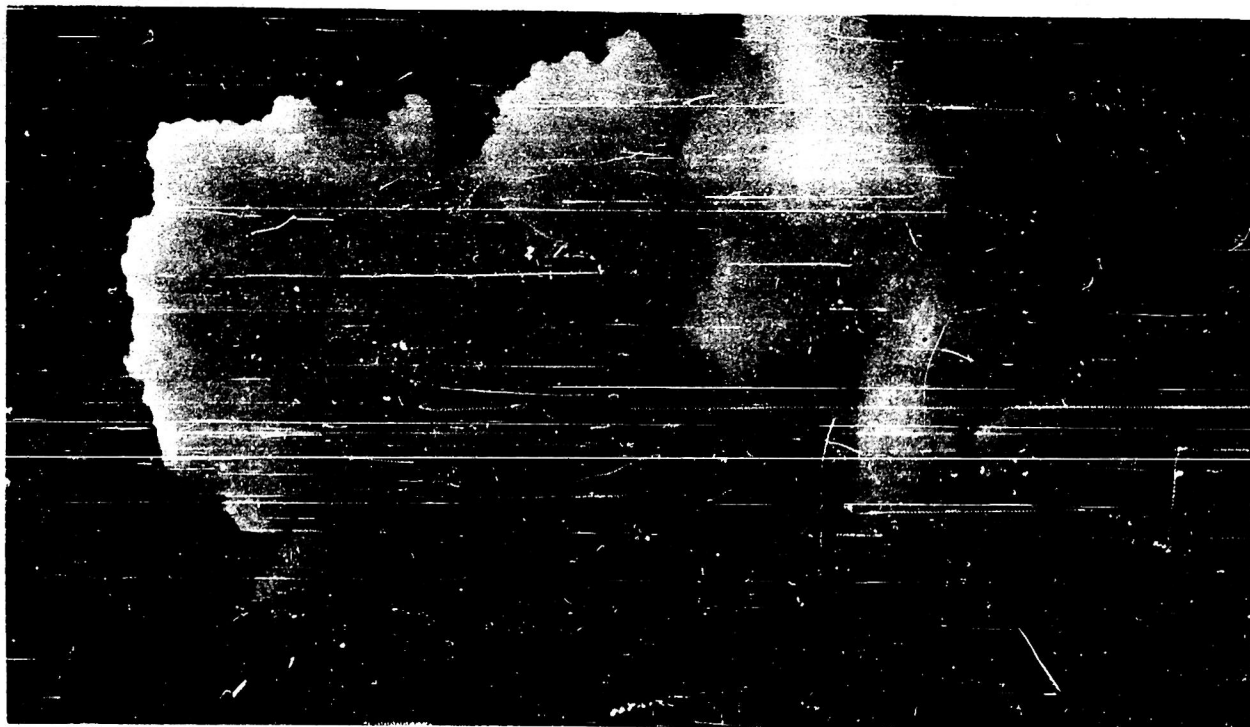
NANTUCKET
AUGUST 14, 1950
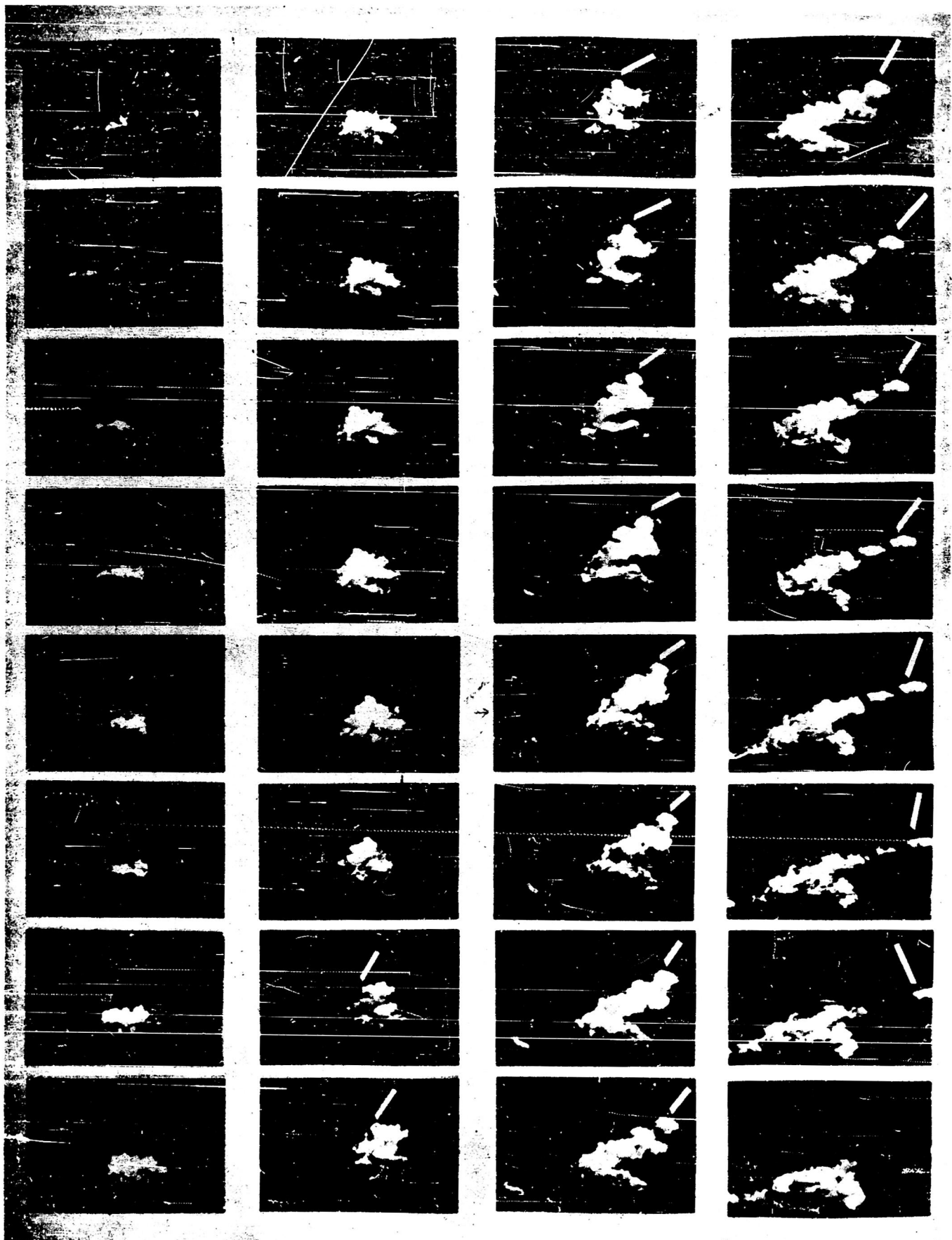
FIG. 4

NANTUCKET
AUGUST 14,1950

HEIGHTS

2300 M

425
M

1300 M

450 M

FIG. 5

HEIGHT (KM)

Env.
Tv

BUBBLE
Tv

NANTUCKET
AUGUST 14,1950

P
(mb)

700

3
3.2

2600 M

800

2200 M

2.0

4.5

BUBBLE ORIGIN

900
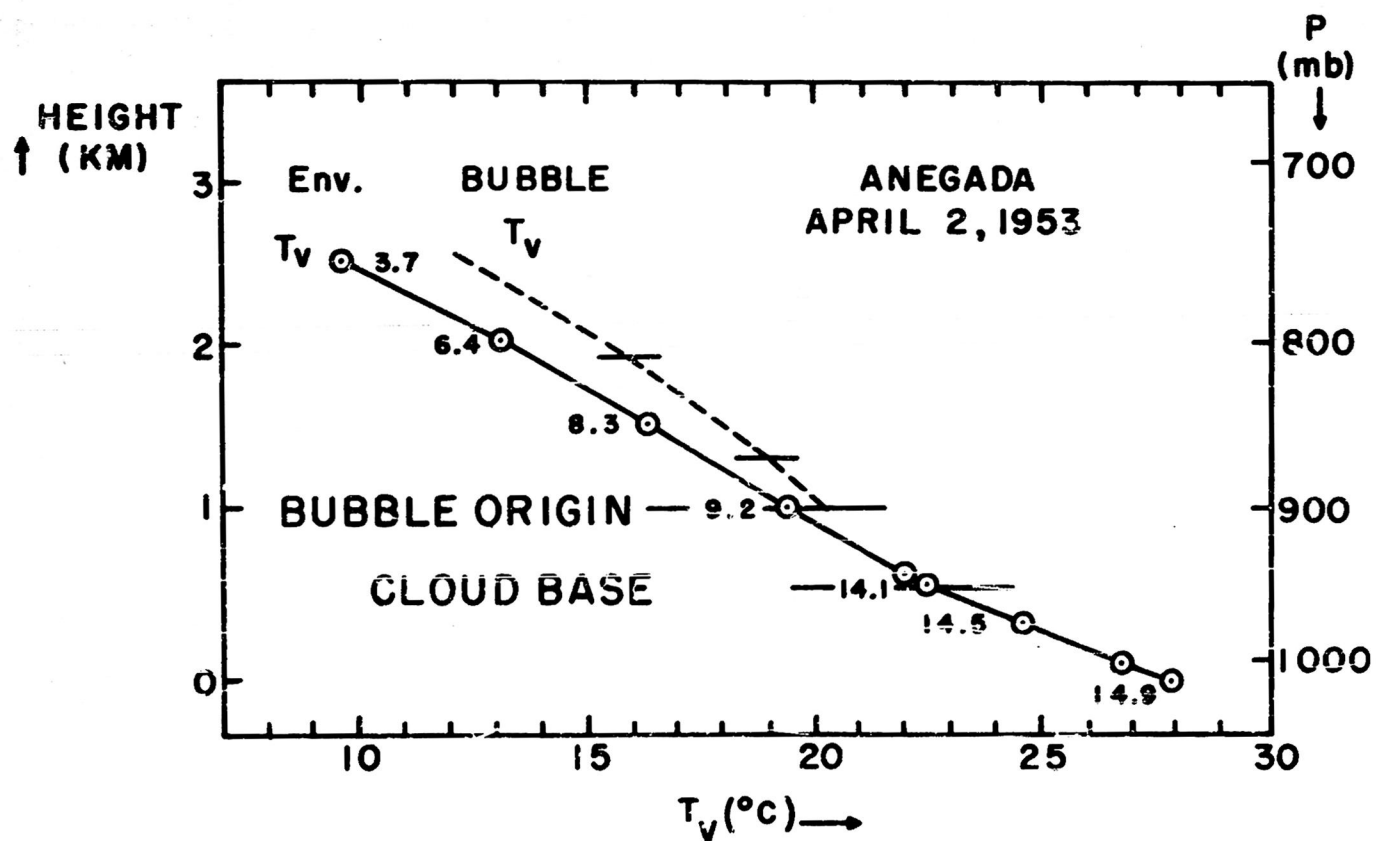
1.0

CLOUD BASE

6.5

9.0

9.1

1000

0.1

10.0

0   5   10   15   20

Tv (°C)
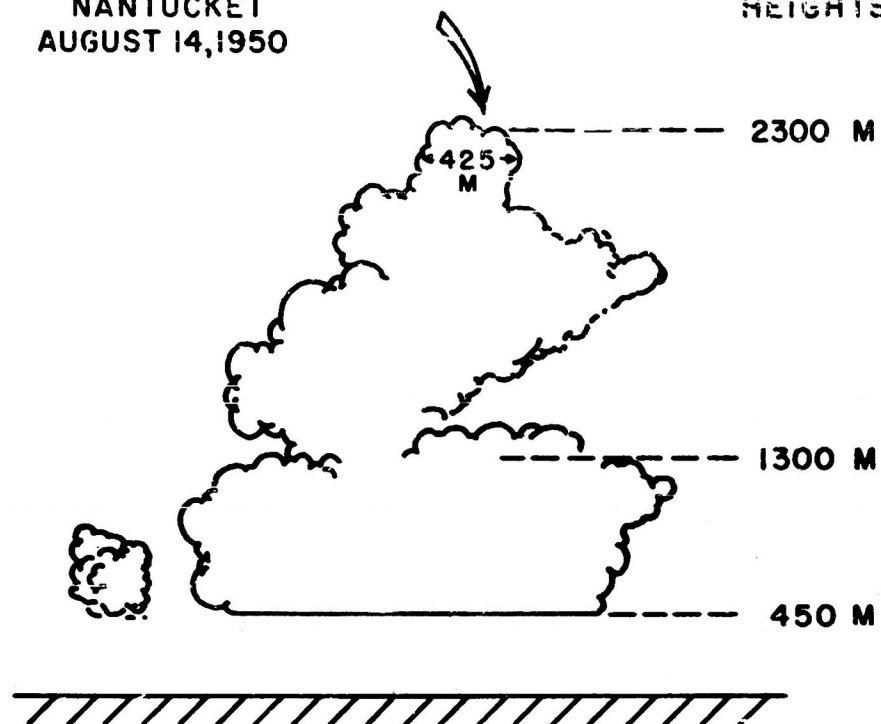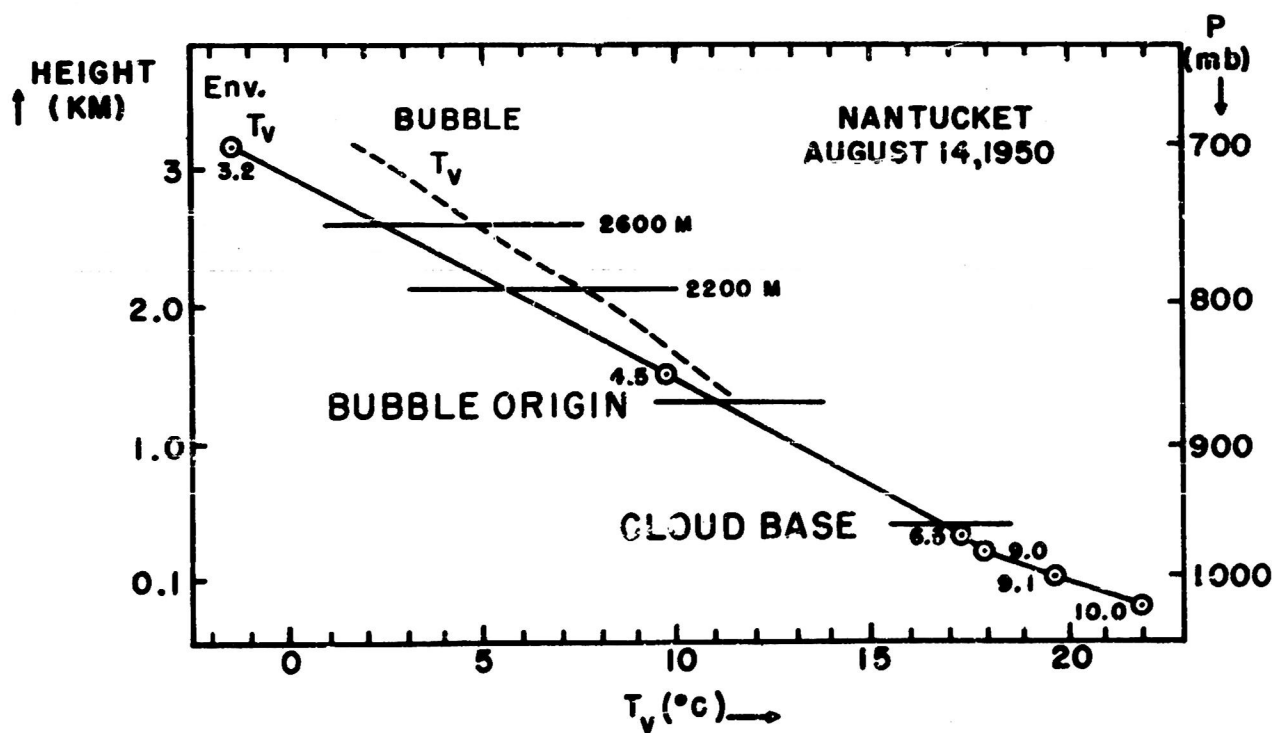
FIG. 6

ST. CROIX
JUNE 30, 1952

HEIGHTS

←750→
M

——— 4450 M

——— 3200 M

——— 1800 M

——— 590 M

FIG. 7

HEIGHT
(KM)

P
(mb)

T$_v$
BUBBLE

T$_v$
Env

ST.CROIX
JUNE 30,1952

BUBBLE ORIGIN

CLOUD BASE

T$_v$ (°C)

FIG. 8

D
(M)

D
(M)

EXPERIMENTAL: $\dfrac{\Delta D}{\Delta t} \cong -4 \times 10^2$

THEORETICAL: $\dfrac{\Delta R}{\Delta t} = -EgB = -50 \times 10 = -5 \times 10^2$

|← 30 SECS →|

183   153   123   93   63   33

(−t) SECS

JUNE 30 1952−ST CROIX
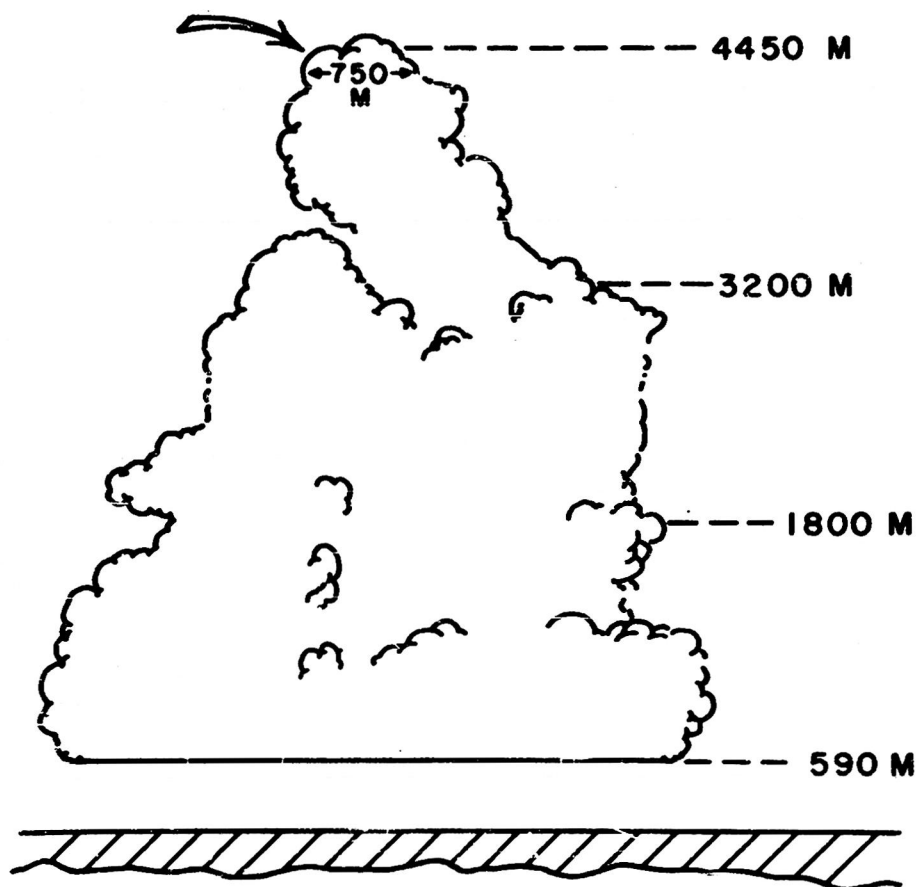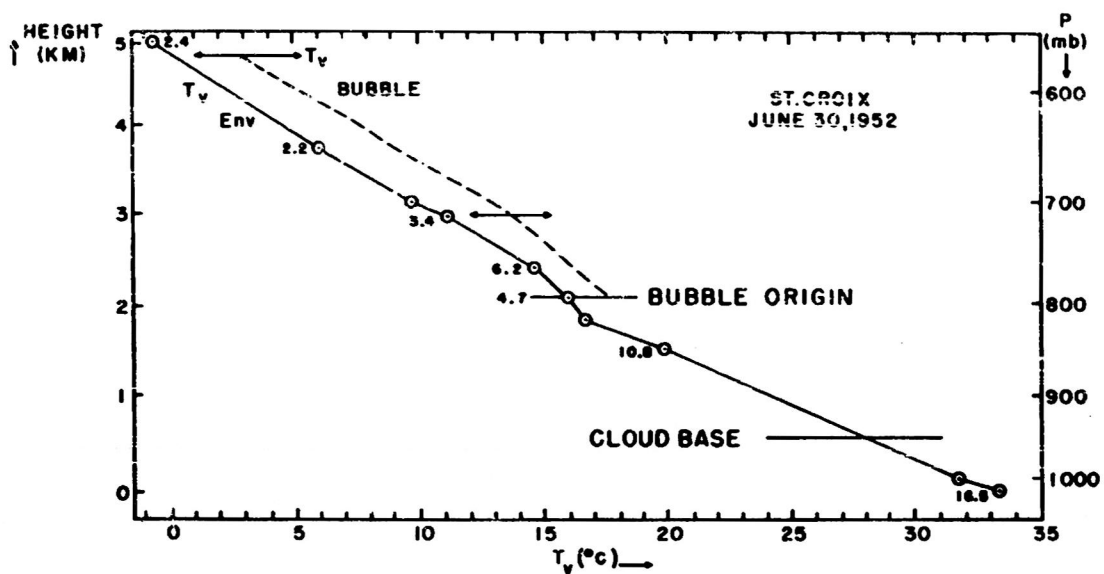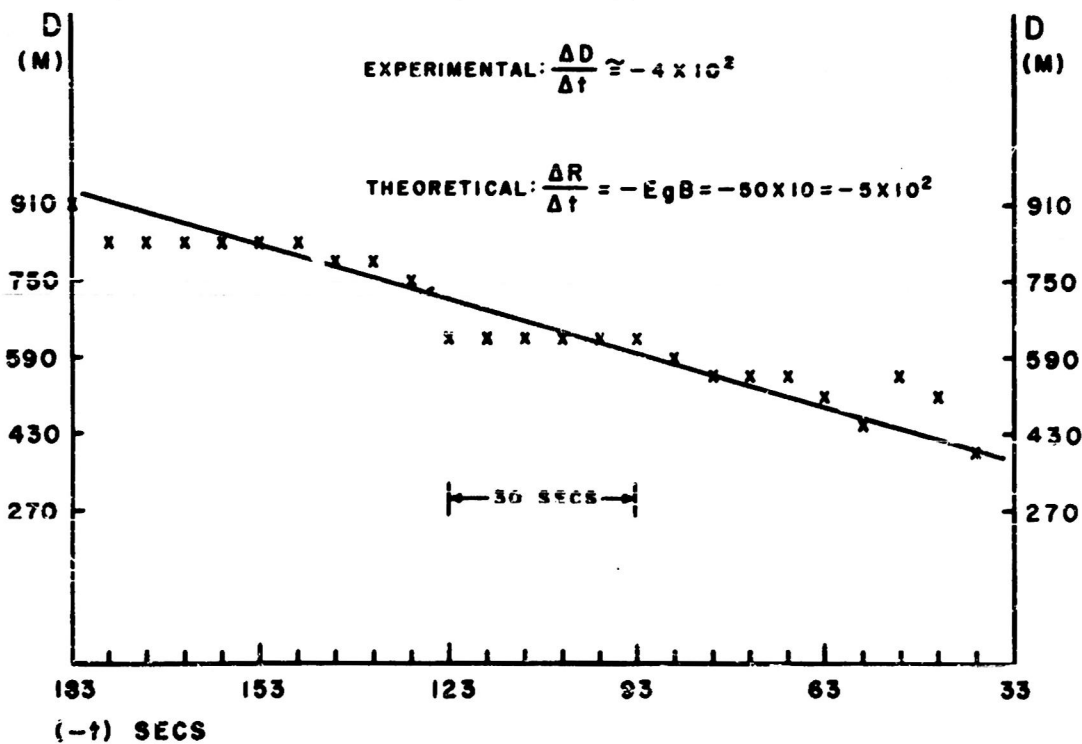
FIG. 9

FIG.10

ANEGADA
MARCH 18, 1953

HEIGHTS

1700 M

2   1   (D ~ 160 M)

570 M

FIG. 11

HEIGHT
↑ (KM)

Ent.
Tv
4.0

a.

BUBBLE
Tv

1

2

ANEGADA
MARCH 18, 1953

P
(mb)

800

2

11.5

13.0

14.0

CLOUD BASE

14.9
15.9

900

1000

1

0

10   15   20   25   30

Tv (°C) ⟶
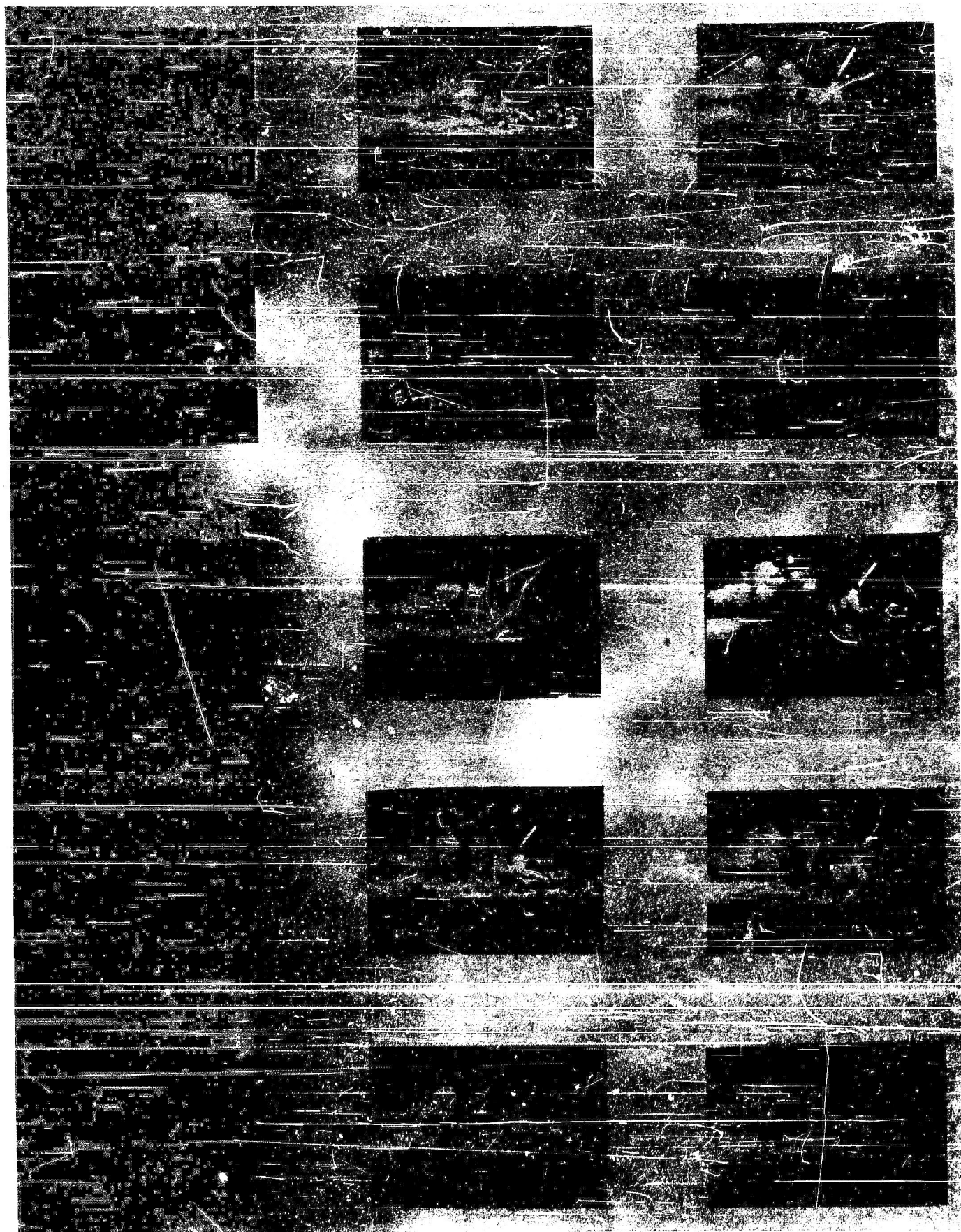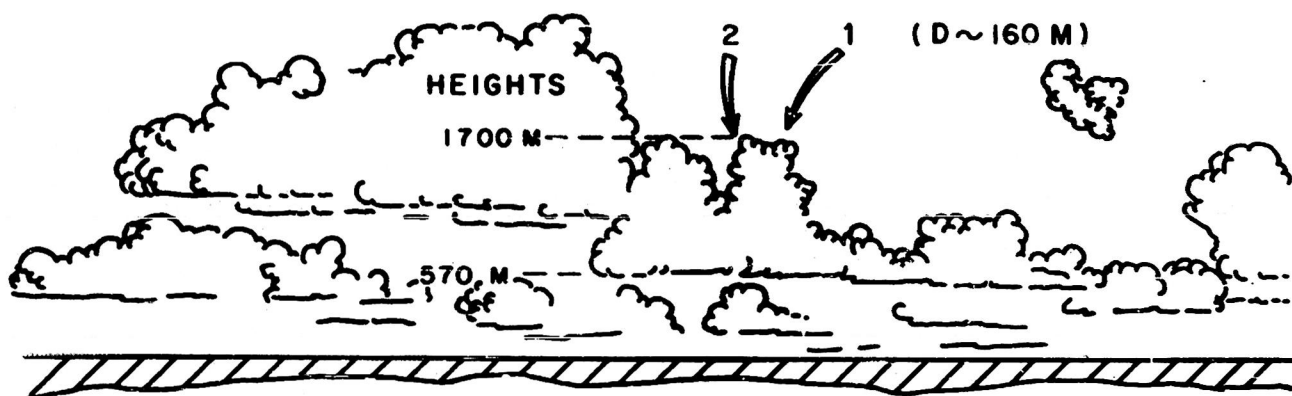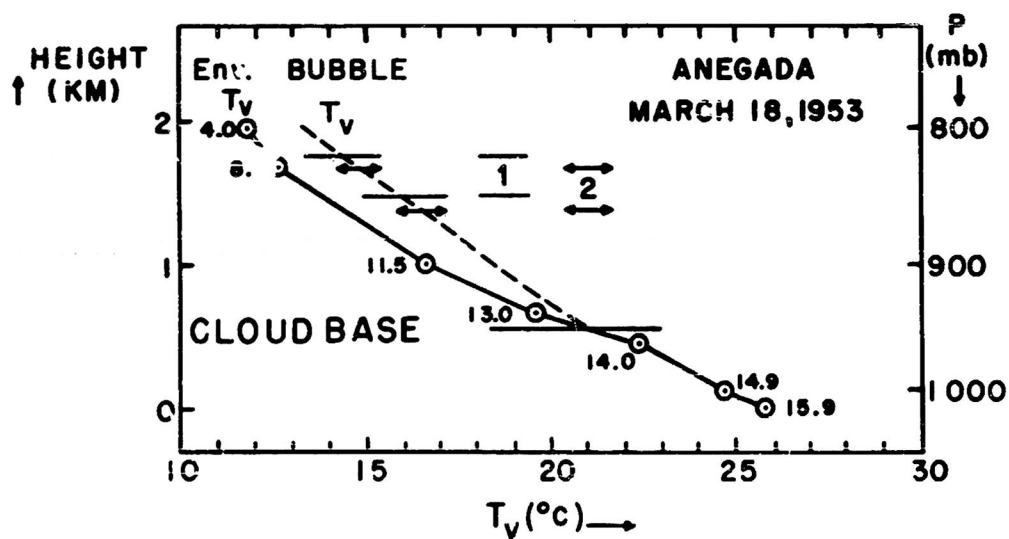
FIG. 12
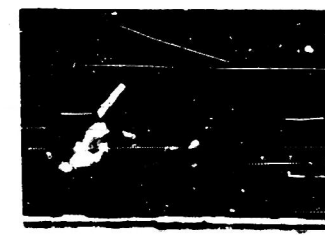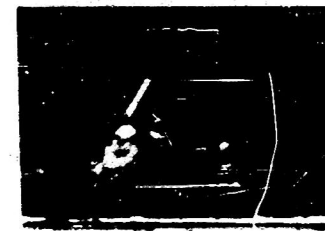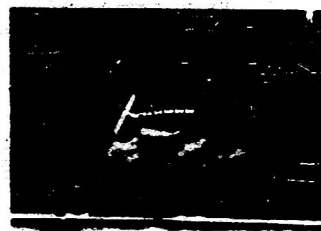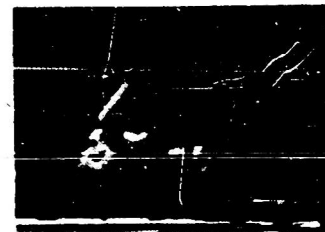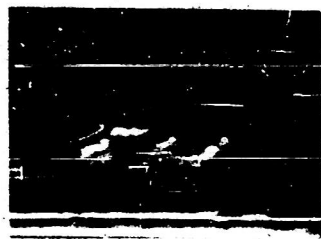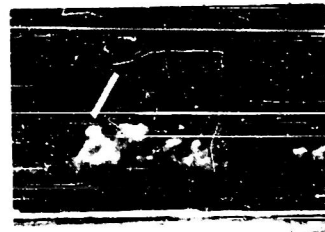
FIG.13

ANEGADA
APRIL 2, 1953

HEIGHTS

1750 M ----
290 M

590 M
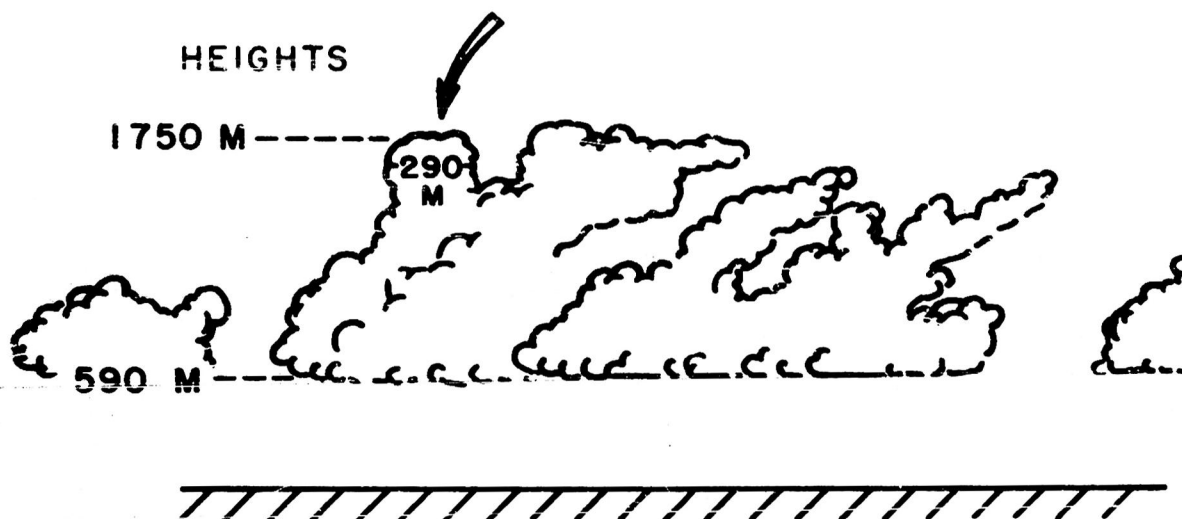
FIG. 14

FIG. 15
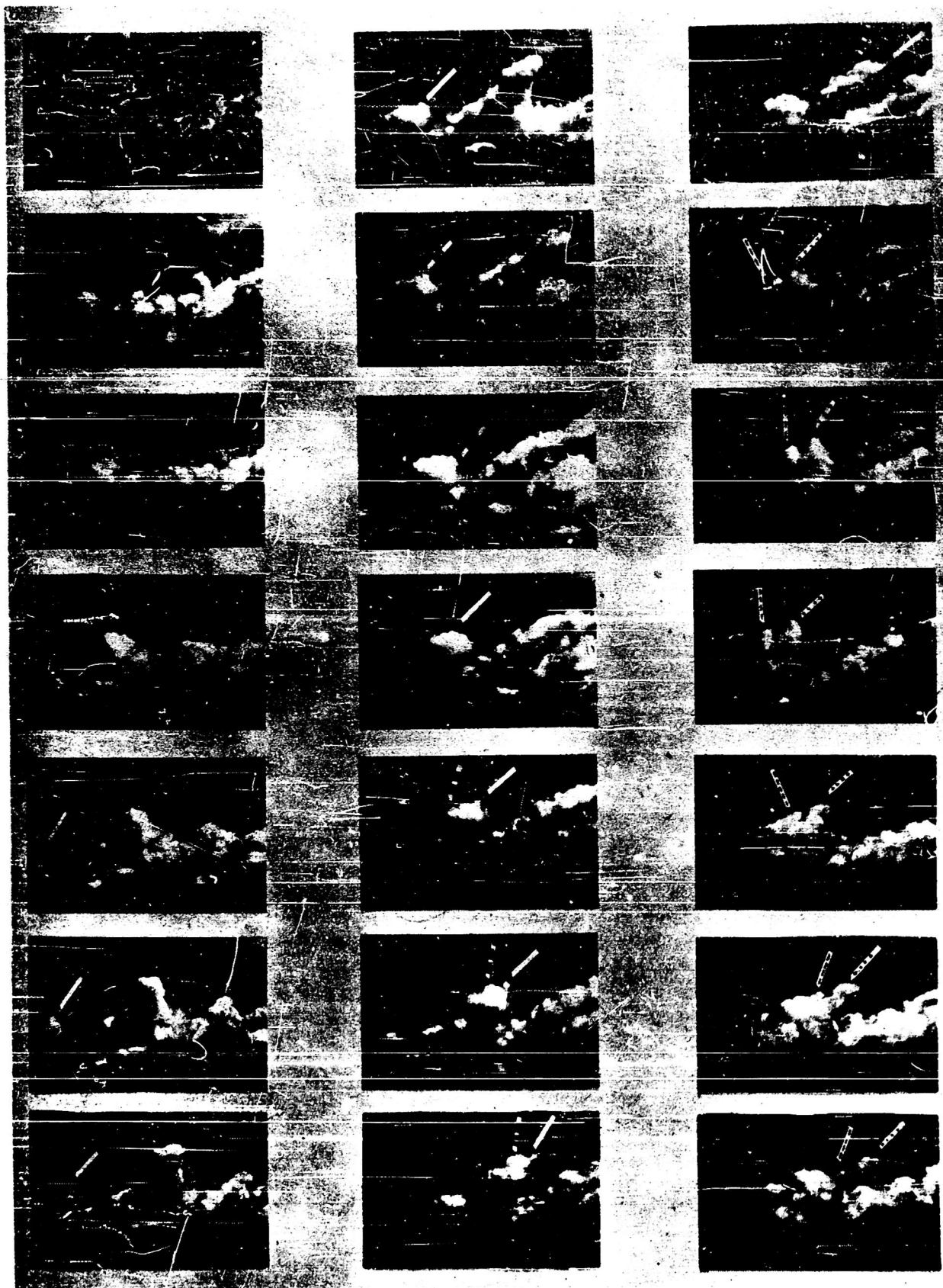
FIG.16

NANTUCKET
AUGUST 8, 1950
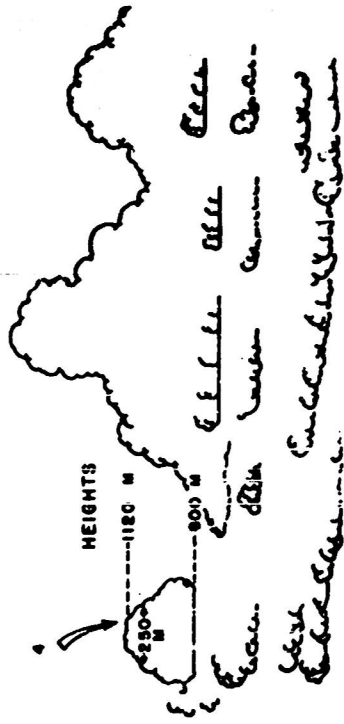
HEIGHTS
1180 M
800 M

A

NANTUCKET
AUGUST 8, 1950

HEIGHTS
1500 M
800 M

COMPOSITE

B

NANTUCKET
AUGUST 8, 1950

HEIGHTS
1600 M
800 M

COMPOSITE
(D~200 M)

C

NANTUCKET
AUGUST 8, 1950

HEIGHTS
1770 M
800 M

D

FIG. 17

FIG. 18

BUBBLE CAP

WAKE

$D \cong 1.0\,R$

$0.5R$

R

θ_m θ_m

$\theta_m = SIN^{-1}\,0.5$

$2\,\theta_m \cong 60°$

FIG. 19

NANTUCKET
AUGUST 8, 1950

COMPOSITE BUBBLE

COMPOSITE BUBBLE

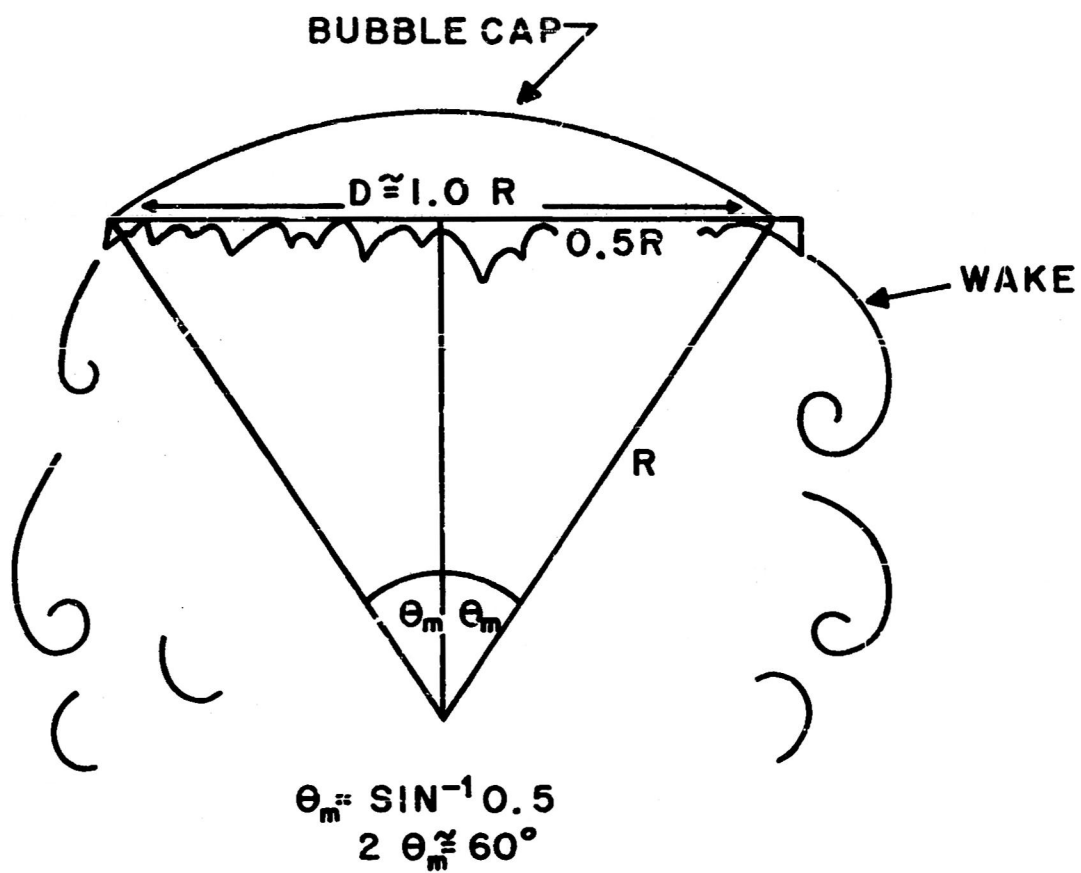HEIGHT (M)

HEIGHT (M)

−t (SECS) FOR COMPOSITE BUBBLE

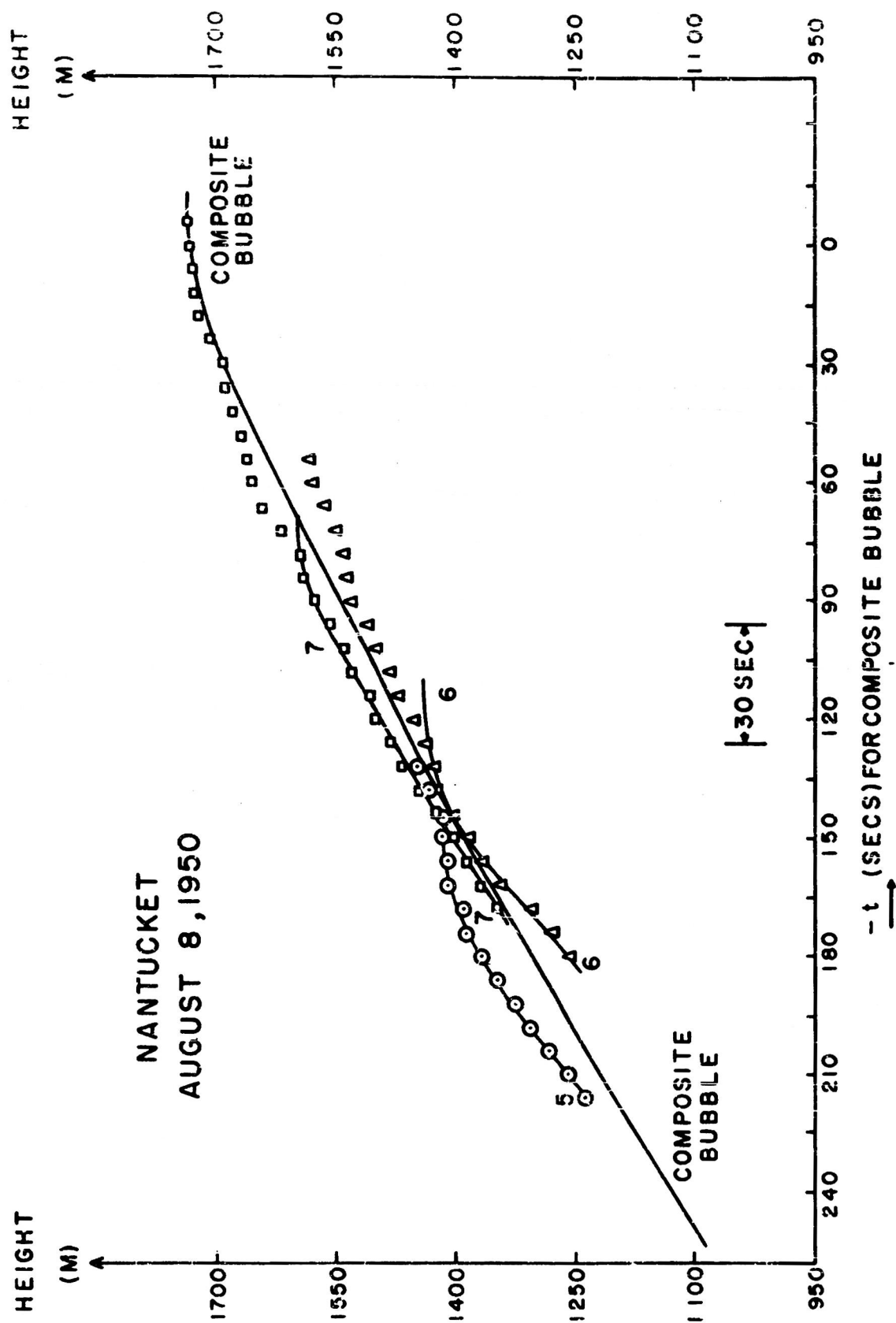|−30 SEC−|
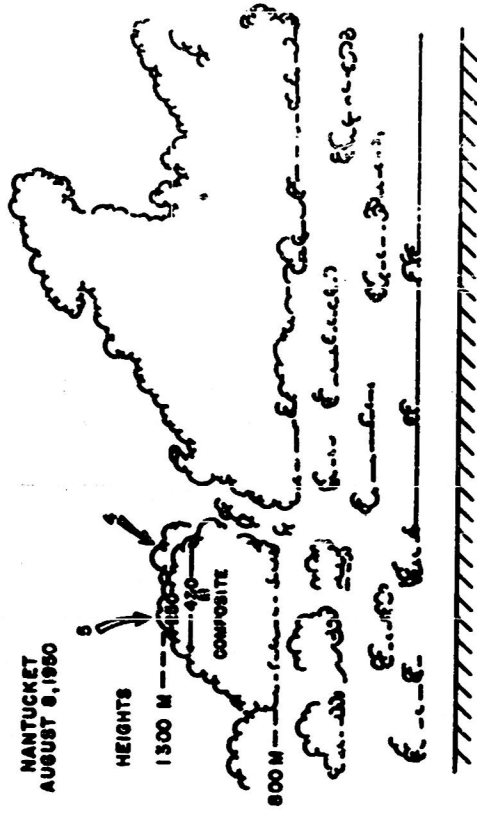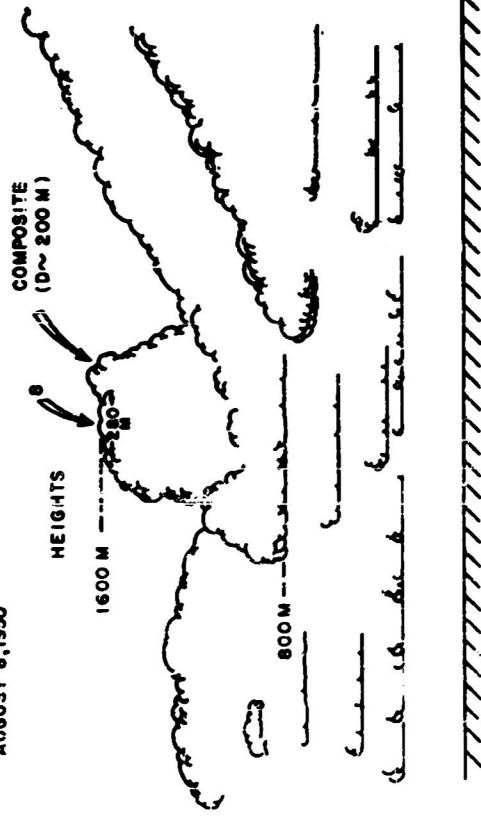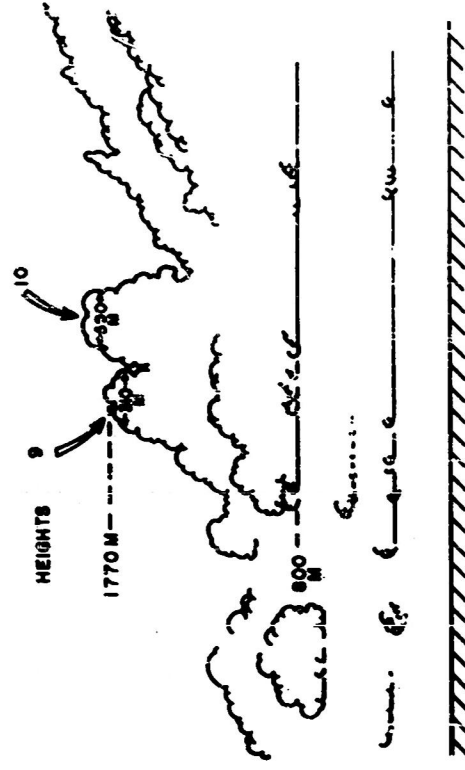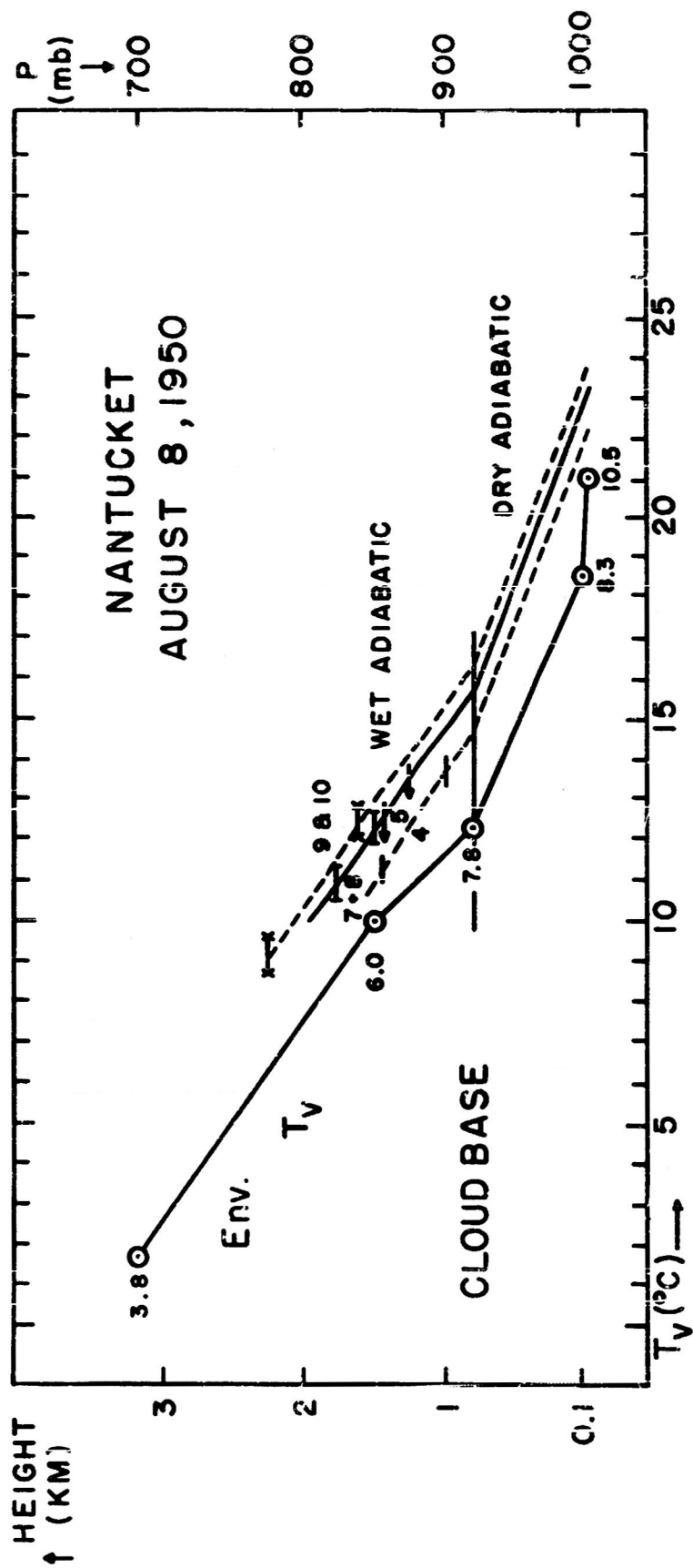
FIG.20

Titles for Illustrations

Fig. 1. Schematic diagram showing the spherical upper surface of a buoyant
bubble of radius of curvature, R. The coordinates are shifted so that
the bubble is at rest and the surrounding fluid has an undisturbed ve-
locity w_0 equal and opposite to its rate of rise. The curve B is the
bubble's upper surface, O is the stagnation point, and A is any point
at an angle θ from the axis of symmetry. The vertical distance between
A and O is x; x' is an extension of R so that the angle between x' and
x is equal to θ.

Fig. 2. Comparison of the atomic bomb cloud and a single trade cumulus
bubble. (After Sutton, 1947).

Fig. 3. Sequence from the time-lapse film of August 14, 1950, showing the
life history of a cloud formed over Nantucket Island, U.S.A. Frames are
reproduced every 30 seconds. Time runs forward down each column, begin-
ning in the upper left corner. The bubble studied is indicated by the
white arrow. Cloud base was at 450 m and the tops reached about 2400 m.
The camera was pointing nearly due east, at right angles to the surface
wind which was from the south (right), decreasing rapidly upward. The
diameter of the bubble was measured on the fourth frame from the bottom,
next-to-right-hand column. This frame corresponds to the drawing in
Fig. 5 and observation 2, Table I.

Fig. 4. Main curve shows the height as a function of time for the bubble
indicated in Fig. 3. Points correspond to each frame on the film (3
seconds apart) and tabulations were made every fourth point (12 seconds

apart). Vertical velocities were obtained from a smoothed curve of the first differences of these heights and accelerations from a smoothed curve of the second differences. The latter curve is shown in the inset graph, with the units converted to c.g.s. The negative of the acceleration, $\Delta w/\Delta t$, is plotted for convenience.

Fig. 5. Tracing of the frame from the time-lapse film corresponding to observation 2, Table I. This is the fourth frame from the bottom, next-to-right-hand column of Fig. 3. The diameter of the bubble was measured on this frame. The height and distance scale was obtained from knowledge of cloud base height from airplane measurements on this cloud simultaneous to the film.

Fig. 6. Diagram showing virtual temperature, T_v, of bubble and environment, as a function of pressure and height on August 14, 1950. The virtual temperature of the environment is indicated by the solid curve. The mixing ratios are entered beside each point in gm/kgm. The solid curve was calculated from the Nantucket radiosonde, made 5 miles from the cloud one hour earlier. The dashed curve is the virtual temperature of the bubble, calculated in the manner described in the text.

Fig. 7. Tracing from the time-lapse film made from St. Croix, June 30, 1952. The film lacked sufficient contrast for reproduction. The tracing was made from the frame corresponding to observation 8, Table II, when the diameter of the bubble (indicated by arrow) was measured. The height and distance scale was determined from the film and simultaneous airplane determination of cloud base height. The camera was

- 63 -

pointed almost due south, and the wind blew from the east (left to right).

Fig. 8.   Diagram showing virtual temperatures, T_v, of bubble and environment, June 30, 1952, as a function of pressure and height. The virtual temperature of the environment is shown by the solid curve, calculated from an airplane sounding together with the San Juan radiosonde (at high levels). Mixing ratios are indicated in gm/kgm next to each point. The virtual temperature of the bubble is given by the dashed curve and was computed as described within the text. The horizontal arrows on the dashed curve delimit the height range in which the bubble was studied.

Fig. 9.   Diameter of bubble as a function of time, St. Croix, June 30, 1952. The times correspond to those in Table II with t = 0 at the bubble's demise.

Fig. 10. Sequence from the Anegada time-lapse motion picture film, March 18, 1953. Frames are reproduced every 36 seconds. Time runs forward down each column, beginning in the upper left corner. The tower containing the bubbles studied is denoted on each frame by the single white arrow. The two bubbles used are indicated by the two arrows in the center frame. This frame is traced in Fig. 11, at which time the diameters of the bubbles were measured. This frame corresponds to observation 5, Table III, and observation 1, Table IV. The camera was pointed nearly due north, and the wind was easterly (from right to left), with little shear. Cloud base was determined by simultaneous airplane observation to be 570 m.

Fig. 11. Tracing of the frame from the time-lapse film, March 18, 1953,
corresponding to the central frame on Fig. 10, observation 5, Table
III, and observation 1, Table IV. The diameters of the bubbles were
estimated roughly from this frame. The height scale was obtained
from the film using airplane observations of cloud location and height
of cloud base.

Fig. 12. Diagram showing virtual temperatures, T_v, of bubbles and environ-
ment, March 18, 1953, as a function of pressure and height. The en-
vironment virtual temperature (solid curve) was calculated from an air-
plane sounding made in the clear near the clouds studied, simultane-
ously to the photographs. Mixing ratios are given in gm/kgm next to
each point. The virtual temperatures of the bubbles (dashed curve)
were calculated in the manner described in the text.

Fig. 13. Sequence from the time-lapse film made from Anegada, April 2,
1953. The bubble studied is indicated by the white arrow. Frames are
reproduced every 36 seconds. Time runs forward down each column be-
ginning in the upper left corner. The bottom frame in the left-hand
column is traced in Fig. 14 and corresponds to observation 8, Table V.
Cloud base was determined by airplane measurements to be at 590 m.
The camera was pointed almost due north and the wind is easterly (right
to left).

Fig. 14. Tracing of the frame from the time-lapse film, April 2, 1953, on
which the diameter of the bubble was measured. This frame is the bot-
tom left-hand frame of Fig. 13 and corresponds to observation 8, Table

- 65 -

V. The height and distance scale was determined from the film together
with airplane determination of cloud base height.

Fig. 15. Diagram showing virtual temperatures, T_v, of bubble and environ-
ment on April 2, 1953, as a function of pressure and height. The vir-
tual temperature of the environment is indicated by the solid curve and
was obtained from an airplane sounding made in the clear air near the
clouds simultaneously with the photographs. Mixing ratios in gm/kgm
are indicated next to each point. The virtual temperature of the bubble
is shown by the dotted curve, which was calculated as described in the
text. The height range of the bubble covered by the calculations is in-
dicated by the two solid horizontal lines crossing the dotted curve.

Fig. 16. Sequence from the time-lapse film of August 8, 1950, showing the
bubbles formed over Nantucket Island, U.S.A. Frames are reproduced
every 30 seconds. Time runs forward down each column, beginning in the
upper left corner. Bubble 4 is indicated by the first white arrow, com-
mencing in the third-from-bottom frame, column 1. Bubble 5 is indicated
by the arrow containing a single black band. Bubble 7 is denoted by
the next white arrow, while bubble 8 is indicated by the arrow with the
two black bands. Bubble 9 is indicated by the arrow containing black
dashes, while bubble 10 is marked by the arrow containing black dots.
The diameter of bubble 4 was measured on the frame where the arrow de-
noting it first appears (observation 2, Table VI). Bubble 5's diame-
ter was obtained from the top frame, middle column (observation 2,
Table VII); the diameter of bubble 8 was determined from the next-to-
bottom frame, middle column (observation 3, Table IX); the diameter

of bubble 9 was obtained from the next-to-top frame, last column (observation 4, Table X) and the diameter of bubble 10 from the next frame below (observation 3, Table XI). Cloud base height was determined to be 800 m from airplane observations simultaneous to the photography. The camera was pointed nearly due east and the wind was from the north (left to right) with moderate positive shear.

Fig. 17.

a. Tracing from the time-lapse film August 8, 1950, showing bubble 4 at the time its diameter was measured (first white arrow, Fig. 16) corresponding to observation 2, Table VI. The height and distance scale was determined by film and airplane measurement of cloud base height.

b. Tracing from time-lapse film, August 8, 1950, corresponding to top frame, column 2, Fig. 16, at which diameter of bubble 5 was measured (observation 2, Table VII). Also appearing on this frame are bubble 4 in its last stages, and the composite bubble (see Table XIII). This is not the frame at which the diameter of the composite bubble was measured.

c. Tracing from time-lapse film, August 8, 1950, corresponding to the second-from-bottom frame, Fig. 16, at which the diameter of bubble 8 was measured (observation 3, Table IX). Also appearing is the composite bubble, whose diameter has shrunk to 200 m at this stage.

d. Tracing from the time-lapse film August 8, 1950, corresponding to the second-from-top frame, column 2, Fig. 16 at which the diameter of

bubble 9 was measured (observation 4, Table X). Also appearing is
bubble 10, whose diameter is given here corresponding to observa-
tion 3, Table XI, although the actual measurement was made slightly
later.

Fig. 18. Diagram showing virtual temperatures, T_v, of bubbles and environ-
ment, August 8, 1950, as a function of pressure and height. The en-
vironment virtual temperature is given by the left-hand solid curve,
which was calculated from the Nantucket radiosonde observation made
near the time of the photographs and within 8 miles of the clouds.
The mixing ratios are given in gm/kgm beside each point. The virtual
temperature curve for bubble 4 is given by the left-hand dashed curve,
the height range studied being indicated by solid horizontal lines.
The virtual temperatures for bubbles 5, 7, and 8 are given by the
right-hand solid curve. The height range for bubble 5 is indicated by
the arrows and for bubbles 7 and 8 by the solid lines with bars at each
end. The virtual temperatures for bubbles 9 and 10 are given by the
right-hand dashed curve and the limits of study are denoted by solid
horizontal lines with x's at each end. The bubble virtual temperatures
were calculated in the manner described in the text. The bubbles each
followed a dry adiabat up to cloud base and a moist adiabat from thence
upward. Although the warmest bubbles (9 and 10) had a surface virtual
temperature nearly $3^{\circ}C$ in excess of the value from the radiosonde,
study of the hourly sequences at Nantucket airport revealed a maximum
temperature (actual) within $0.2^{\circ}C$ of the actual temperature required
by these bubbles.

- 68 -

Fig. 19. Schematic diagram of an isolated bubble, drawn to resemble the
bubbles studied by Davies and Taylor (1950). The bubble has a spheri-
cal cap, a flat but very irregular lower surface, and a turbulent wake
behind it. The radius of curvature of the spherical cap is denoted by
R, and the diameter of the spherical cap by D. They are related by the
equation $\sin \theta_m = D/2R$, where θ_m is one-half the total angular aperture
of the bubble cap. The average bubble studied was found to have a
diameter $D \cong 1.0\ R$, or an angular aperture of 60°, at the lower limit
of the range of air bubbles in liquid studied by Davies and Taylor
(1950).

Fig. 20. The height-time curve for bubbles 5, 6, and 7, August 8, 1950 and
for the composite bubble formed by these individuals. The curve for
the composite bubble was drawn using the points on this figure and was
checked on the film by tracking the smoothed upper outline of the large
tower dominating column 2, Fig. 16, which was in fact the composite
bubble.